DEPARTMENT OF INTERNATIONAL AND EUROPEAN ECONOMIC STUDIES

ATHENS UNIVERSITY OF ECONOMICS AND BUSINESS

Economic Growth and the Environment: A Theoretical Reappraisal

Maxime Menuet

Alexandru Minea

Patrick Villieu

Anastasios Xepapadeas

Working Paper Series

20-31

August 2020

Economic Growth and the Environment:
A Theoretical Reappraisal

Maxime Menuet[a], Alexandru Minea[b,c], Patrick Villieu[a], Anastasios Xepapadeas[d,e,*]

[a] *University of Orleans, CNRS, LEO, Orléans, France*
[b] *CERDI and School of Economics, University Clermont Auvergne, France*
[c] *Department of Economics, Carleton University, Canada*
[d] *Athens University of Economics and Business, Greece*
[e] *Department of Economics, University of Bologna, Italy*

Abstract

The relationship between economic growth and the environment is at the core of the theoretical and empirical researches since at least thirty years. This paper shows that a small-dimension ecological growth model can lead to a great diversity of relationships between pollution and growth, including the popular environmental Kuznets curve (EKC) and logistic curve (ELC). We exhibit multiple equilibria and complex local and global dynamics resulting in potential indeterminacy or long-lasting pollution cycles. Furthermore, our model reveals an ecological poverty trap associated with a possible irreversibility of the environmental degradation. Interestingly, our findings do not resort on some exogenous technological breaks but result from the endogenous interaction between households' saving behaviour and the natural resources' law of motion.

Keywords: Growth, Environment, Bifurcation, Endogenous Cycles, Poverty Traps, Pollution

JEL Codes: E32, O44, Q50

1. Introduction

The interaction between economic growth and environmental quality has been the subject of a large debate over the last few years. Much of the empirical studies focused on the relationship between per capita income and various types of polluting emissions (see, e.g., World Bank, 1992; Selden and Song, 1994; Grossman and Krueger, 1995, among others). Following the pioneer work of Grossman and Krueger (1995), the *environmental Kuznets curve* (EKC) became a major concept to describe the evolution of polluting emission along the development process. According to the EKC, in the early stages of economic growth, emissions increase and environment quality declines, while this effect reverses above some economic development threshold, such that—at high levels of income—economic growth and pollution emissions are negatively linked.

The EKC has been applied to a large range of pollutants, exhibiting a wide variety of empirical findings. In their meta-analysis, Pérez-Suárez and López-Menéndez (2015)

*Corresponding author: Email: xepapad@aueb.gr.

found that the Kuznets inverted-U shape between emissions and the level of per capita income is supported by 55.7% of the studies, while more non-monotonic patterns are accounted in 17.7% of the cases. However, evidence against the EKC—showing increasing trends between emissions and the per capita income—is reported for 11.5% of the studies.

The latter effect refers to the possibility of an *environmental logistic curve* (ELC). The explanatory power of the logistic function has already been highlighted in a wide range of fields, including demography, biology, or medicine. As regards environment, the ELC suggests that polluting emissions are approximately exponential at the initial stage of development; then, a saturation begins making the pollution to slow down, and at maturity it stops. This pattern differs from the EKC at high income levels, since pollution emissions are stabilizing but do not decline.[1] Several empirical findings are consistent with the ELC, in particular for CO2 emissions (Shafik, 1994; Jaunky, 2011; Kaika and Zervas, 2013); using data for 175 countries during the 1860-2012 period, Pérez-Suárez and López-Menéndez (2015) show that the EKC model is the most suitable in 44% of the countries, while the ELC outperforms it in 24% of the countries, and the two models are similar in 17.6% of the countries.[2]

Altogether, it is clear that there is a great diversity in the time profile of CO_2 emissions, as illustrate by Figure 1. Sweden and Finland follow an EKC and an ELC respectively. However aside from the EKC and the ELC, more complex scenarios can occur in both developed and developing countries. For example, CO_2 emissions seem to follow a long-lasting cyclical dynamic in Denmark, while they have fallen since the 1990s in Congo. From a theoretical standpoint, these features could suggest the existence of a limit-cycle or a no-growth trap.

Beyond possible statistical pitfalls (see the impressive survey of Stern, 2006), the considerable empirical literature on the EKC also suffers from weak underlying theoretical foundations. As pointed out by Grossman and Krueger (1995), the EKC is a reduced-form equation that measures the relation between income and polluting emissions but says nothing about the intrinsic structural functions of the economic system that lead to this relationship. Even if a number of theoretical works support the existence of the EKC (notably following different hypotheses on preferences or technology, as recalled below), these contributions may require for a reappraisal because "*if the EKC for emissions is monotonic as more recent evidence suggests, the ability of a model to produce an inverted U-shaped curve is not a particularly desirable property*" (Stern, 2004).

[1]The EKC and the ELC are consistent with the theoretical assumption that polluting emissions are constant in the long-run. These two curves merely describe the dynamics of emissions along the development process, before the economies reach their potential long-run equilibrium.

[2]Notice that the ECK and the ELC can be reconciled if we consider a marginal EKC, namely an inverted U-shaped curve between the marginal increase of emissions and the level of income. In this case, the relation between emissions and the level of income will take the form of a logistic curve (see, e.g., Sobhee, 2004).

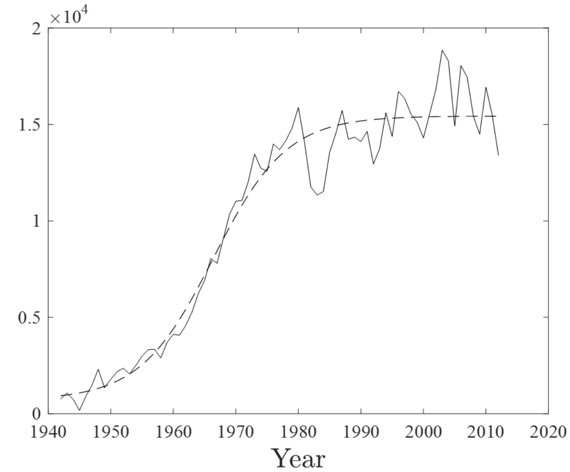

1a. Finland

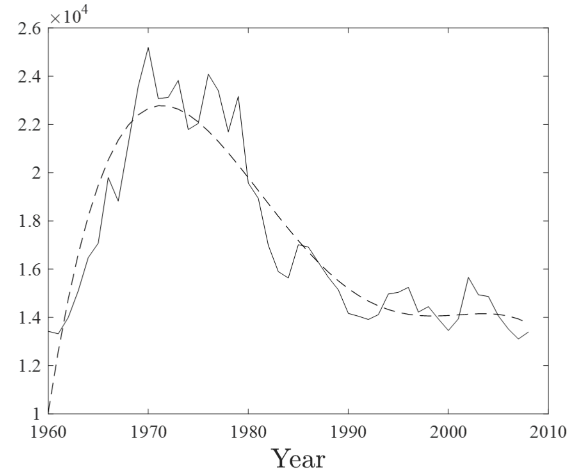

1b. Sweden

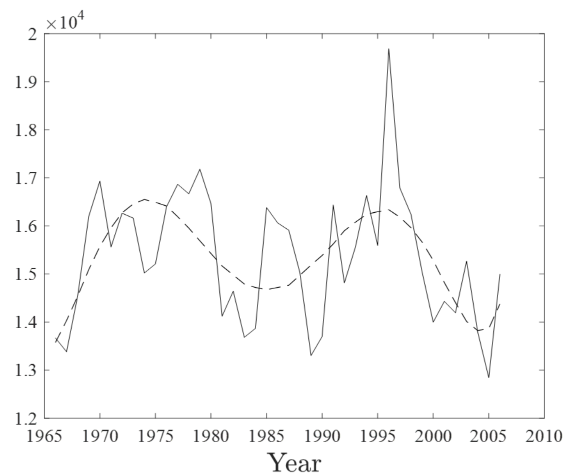

1c. Denmark

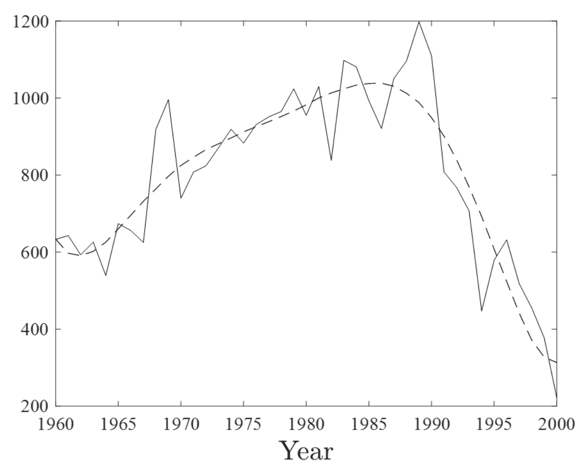

1d. Democratic Republic of Congo

Figure 1: Time profile of CO_2 emissions for a selection of countries
(metric tons of CO_2, Carbon Dioxide Information Analysis Center, 2014)

The goal of this paper is precisely to develop a theoretical setup that is able to provide various types of relations between the environment and economic growth—including the popular environmental Kuznets and logistic curves—based on usual assumptions. As we are concerned by long-run relationships and due to the lack of robust evidence on income convergence among nations (Durlauf et al., 2005), we build an environmental endogenous growth model. We model environmental quality as a stock of natural capital that positively affects both households' utility and the total factor productivity. Following Tahvonen and Kuuluvainen (1991) and Bovenberg and Smulders (1995), the stock of natural capital is depicted as a renewable resource that accumulates due to the nature's regenerative capacity and depreciates with pollution—viewed as the extractive use of natural resources for productive services. Thanks to investment in abatement knowledge (here provided by public spending), economic growth and environmental preservation can be compatible in the long-run.[3] Therefore, "pollution-saving" technologies challenge the claim that environment and economic growth are necessarily negatively related in the long-run. If e.g. pollution damages the very engine of growth, i.e. human capital accumulation, a cleaner environment—by increasing human capital—leads to a higher rate of growth. In this way, abatement can overcome the conflict between environment and economic growth (Van Ewijk and Van Wijnbergen, 1995).

However, existing environmental growth models are probably too optimistic because they usually focus on an unique balanced-growth path and disregard transitional dynamics. Yet, endogenous growth models often exhibit the possibility of multiple steady-state solutions, which generate non trivial local and global dynamics associated with different transitional paths. Indeed, in general equilibrium the dual interaction between economic growth and the environment can produce complex dynamics, notably because polluting emissions may reversely affects the process of economic growth, as notably pointed out by Arrow et al. (1995). This contrasts, e.g., with the early empirical literature on the EKC that assumed an unidirectional causality running from income to environmental quality.

Our findings.

(1) First, our model exhibits multiple equilibria. Three steady states can appear: a "*dark" equilibrium* characterized by a low economic growth and a low environmental quality; a *"green" equilibrium* with a high growth and a high environmental quality; and an *"intermediate" equilibrium*. Intuitively, the multiplicity of long-run steady-states comes from the reciprocal interaction between economic growth and the environment. A low environmental quality generates low factor productivity that impedes economic growth. Reciprocally, a low economic growth does not ensure enough public spending for abatement, and leads to high emission flows. These mechanisms reverse in the case of a high environmental quality, which conducts to strong economic growth, generating multiple self-fulfilling steady states.

(2) Second, regarding the transitional dynamics, local and global indeterminacy can appear.[4] Indeed, the dark and the green equilibria can be reached by a saddle path, while the intermediate equilibrium can be stable or unstable. Depending on the initial environmental quality and households' expectations, the economy can be trapped in the dark equilibrium (an environmental-poverty trap), converge towards the green steady

[3] Bovenberg and Smulders (1995) provide an exhaustive analysis of the technological conditions under which continued growth is compatible with sustainable regeneration of environmental resources.

[4] As usual in the literature, local indeterminacy refers to an infinity of possible paths towards a given equilibrium and global indeterminacy corresponds to several possible paths towards different equilibria, starting from given initial conditions.

state, or experience oscillating trajectories through endogenous cycles. At the limit, long-lasting endogenous fluctuations can take the form of homoclinic orbits, which define paths that join a steady-state to itself. From a global dynamics perspective, the existence of such orbits are ensured by the occurrence of generic Bogdanov-Takens (BT) bifurcations.[5]

(3) Third, our model can produce many scenarios, including environmental Kuznets or logistic curves, and also pollution cycles or an irreversible trajectory towards the environmental-poverty trap. These different configurations rely on a hysteresis phenomenon reflecting the extreme sensitivity of the long-run solution to changes in parameters. For small changes in the environmental tax, for example, the steady state may suddenly shift from the green equilibrium to the ecological-poverty trap in a non-reversible way (through the occurrence of a *cusp* bifurcation). Quantitatively, our analysis based on a calibration exercise shows that these different scenarios occur for empirically-plausible values of the variables.

Finally, the main contribution of this paper is methodological. We do not aim to replicate real cases, but we highlight that the dual interaction between growth and environment generally leads to indeterminacy, bifurcations, and complex dynamics (including the EKC and ELC), so that even the most cautious environmental policy can easily lead to unexpected consequences, even in the simplest and most innocuous environmental growth model (in the spirit of Tahvonen and Kuuluvainen, 1991) based on a realistic calibration with standard assumptions.

Related literature.

Although the EKC is an "*essentially empirical phenomenon*" (Stern, 2015), its popularity motivated several strands of theoretical models devoted to the study of the relationship between economic growth and the environment.

A first line of research considers that the EKC results from a regime switch in abatement technology that produces two opposite-sign relations between environment and income. In e.g. Stokey (1998), only dirty technologies are available below some level of income threshold; as such, during the growth process pollution increases with income until the threshold is passed, but then decreases once cleaner technologies can be used. In the overlapping generations model of John and Pecchenino (1994), the emergence of the EKC is based on a break in abatement activity that produces two distinct development stages: in the first stage households favour consumption against the environment, such as economic growth is associated with an increase of polluting emissions; in the second stage—once the economy has reached a sufficient level of wealth or because of important environmental damages—households begin to clean up the environment, and economic

[5] BT bifurcations are equally used by Benhabib et al. (2001) to show the destabilizing features of Taylor monetary rules and—more recently—by Sniekers (2018) regarding the presence of Beveridge cycles in the labor market.

growth becomes consistent with improvements in environmental quality. However, the resulting pollution-income path illustrated by these approaches exhibits a sharp peak when the regime switch occurs, which may be at odds with the smooth adjustment of pollution observed in the data.

A second line of research emphasizes the role of transitional dynamics. By amending the Solow (1956) model to incorporate technological progress in abatement, Brock and Scott Taylor (2010) illustrate an EKC arising from the convergence to the sustainable growth path. Hartman and Kwon (2005) extend the Uzawa (1965)–Lucas (1988) two-sector endogenous growth model with human and physical capital to include pollution, and show that an EKC may appear or not during the transition path depending on parameters—but only with pollution defined as a flow; when the environment is defined as the stock of natural capital, Dinda (2005) exhibits an EKC—however, only off the stable manifold that converges towards the steady state. A comparable result appears in Rubio et al. (2009), who introduce endogenous growth in the Foster (1973)'s model; in addition, since sustained growth characterizes only one of the two equilibria, global dynamics are not analyzed. With respect to this literature, the various shapes of the relationship between environment and income that we unveil are equilibrium-based relationships.

Our model is also related to a third line of research that highlights the role of irreversibility in the pollution-growth nexus. Most of growth models—including ours—assume that Nature assimilates pollutants at a constant rate. Several authors —including notably Dasgupta (1982)—challenge this view and consider that high pollution may drastically alter Nature's assimilation capacity. In this vein, Tahvonen and Salo (1996) and Toman and Withagen (2000), among others, use a decay function with a (exogenous) critical pollution level beyond which pollution accumulation is irreversible (hence, the assimilative capacity of the environment may eventually be exhausted by pollution accumulation); and, more recently, some authors (Mäler et al., 2003; Heijdra and Heijnen, 2013) introduce a smooth assimilation function according to a shallow-lake dynamics. Such functions generate a non-convexity in the optimization problem that—generally—produces multiple equilibria, associated or not with irreversible pollution. On this ground, Prieur (2009) shows in an OLG model that irreversible pollution may challenge the emergence of the EKC. In our model, multiple equilibria rest on neither an exogenous critical pollution level in the decay function, nor a shallow-lake dynamics. On the contrary, irreversibility in the growth-environment relationship arises with a smooth quadratic function of Nature, as in traditional environmental growth models. Importantly, the emergence of the EKC is only one possible shape in our framework, among other possible paths—including a monotonic convergence towards a "green" steady state along an ELC, the trapping of the economy into a "dark" environmental-poverty trap, or long-lasting cyclical dynamics between pollution and economic growth.

Finally, in several papers the existence of the EKC comes from the indeterminacy of equilibria. In a neoclassical growth model with an environmental externality in households' utility function, Fernández et al. (2012) show that self-fulfilling prophecies can generate a non-linear relationships between income and pollution. Assuming a pollution externality in a continuous-time Ramsey economy, Bosi and Desmarchelier (2018a) exhibit a possibly-undetermined unique equilibrium giving rise to an EKC possibly associated to a Hopf bifurcation and a limit-cycle (which may appear on its negatively-sloped branch). With natural resources modeled as a stock, Bosi and Desmarchelier (2018b) obtain two steady-states and show that a limit-cycle can emerge near the higher steady state; besides, rich dynamics and bifurcations can occur, implying large oscillating trajectories in the level of pollution. However, in these papers pollution is a byproduct of economic activity that generates an externality in the household's utility, and there is no economic growth in the long-run.[6] More importantly, the non-separability of consumption and pollution (or natural capital in Bosi and Desmarchelier, 2018b) in the utility function is a fundamental hypothesis for indeterminacy and bifurcations to arise; relatedly, it is the non separability of preferences between consumption and labor that is crucial in Antoci et al. (2011). On the contrary, in our endogenous growth setup with a richer modelling of the impact of the environment—both through pollution as an input and the environmental quality as an externality in the production process—households' preferences are assumed to be *separable* between consumption, labor, and the environment. As such, the novel indeterminacy-channel that we unveil is driven by the impact of the environmental quality on the production function, and the simple interaction between households' optimal saving behavior and the law of natural resource accumulation.[7]

The remainder of the paper is organized as follows. Section 2 presents the model, section 3 computes the equilibrium, section 4 studies the long-run solutions, section 5 performs a quantitative exercise and discusses the various types of bifurcations, section 6 examines the global dynamics and derives the time profile of pollution under different scenarios, and section 7 presents some concluding remarks.

2. The model

We consider a closed economy populated by a continuum of representative individuals whose total measure is 1, and a government. Each representative agent consists of a household and a competitive firm. All agents are infinitely-lived and have perfect foresight. For each variable, we denote individual quantities by lower case letters (x), and aggregate quantities by corresponding upper case letters (X), with $x = X$ at equilibrium since the continuum of agents has unit measure.

[6] Le Kama (2001) and Antoci et al. (2011) introduce an environmental resource as an input to production in an exogenous growth model.

[7] Bosi and Desmarchelier (2019) develop an interesting method to study environmental-growth interactions in dynamic systems of three or four dimensions. Our two-dimension setup—although simpler—equally exhibits rich dynamics and various bifurcations.

2.1. Environment

Environment is modeled as a renewable resource. Following Tahvonen and Kuuluvainen (1991) and Bovenberg and Smulders (1995), the environmental quality (Q_t)—which is the stock of natural capital—accumulates due to the regenerative capacity of Nature and depreciates due to pollution, namely

$$\dot{Q}_t = E(Q_t) - P_t, \tag{1}$$

where a dot over a variable represents a time derivative.

Pollution (P_t) comes from the extraction of natural resources, because production requires pollutant inputs (e.g., pesticides in agriculture, fossil fuels resulting in emissions of carbon, etc.). The mapping $E(\cdot)$ is an environmental regeneration function that reflects the capacity of the environment to absorb pollution. We consider several standard assumptions (see Fullerton and Kim, 2008): $E(\cdot) \in C^1(\mathbb{R}^+)$; there is a critical level $\bar{Q} > 0$ such that $E(\bar{Q}) = 0$; $E(Q_t)$ depicts an inverted U-shaped curve; and $E''(Q_t) \leq 0$. The first assumption models the regeneration process as a smooth function. According to assumption two, without pollution ($P_t = 0$) environmental quality equals its highest possible level: the *virgin state* $\bar{Q}$ that is the maximal stock of natural resources that can be kept intact by natural regeneration, namely $E(\bar{Q}) = P = 0$; however, the steady-state occurs for a strictly positive pollution level in our model—namely $P^* = E(Q^*) > 0$—such as $E(Q^*)$ measures the absorption capacity of the environment.[8] With assumption three, the absorption capacity initially increases with the environmental quality, but then decreases as the environment is getting closer to the virgin state (see also e.g. Bovenberg and Smulders, 1995; Smulders, 2000; Fullerton and Kim, 2008). Finally, the usual decreasing returns of the environmental regeneration process are ensured by the fourth assumption.

2.2. Firms

Output of the representative firm (y_t) is produced using three inputs: private man-made capital (k_t), human capital (h_t), and a polluting input (z_t) that reflects the effective input of "harvested" environmental resources, according to the following production function

$$y_t = A_t k_t^{\alpha} h_t^{\beta} z_t^{\phi}, \tag{2}$$

where A_t is a productivity factor. $\alpha \in (0, 1)$, $\beta \in (0, 1)$, and $\phi \in (0, \alpha)$ are the elasticity of output to private capital, human capital, and polluting input, respectively. The assumption $\alpha > \phi$ ensures normal factor demand functions.[9]

[8] Sustainable development ($\dot{Q}_t = 0$) requires pollution to be constant and not above the maximal absorption capacity in the long run.

[9] $\alpha > \phi$ is a (unnecessary) sufficient condition to ensure that global externalities are small enough for the factor demands to negatively depend on prices.

Four assumptions are made. First, following Romer (1986), human capital is produced both by raw labor (or training activity) l_t, and by the economy-wide stock of capital K_t,[10] namely $h_t = l_t K_t$. Second, we consider that the stock of environmental quality—or natural capital, Q_t—exerts a positive externality through the productivity factor, namely $A_t = A(Q_t)$, where $A' > 0$. Indeed, clean soil, air, or water provide productive services to economic activities, by improving workers' health and productivity, for example.[11] Third, following de Mooij and Bovenberg (1997) and Fullerton and Kim (2008), the input z_t depicts the "effective emissions" that can be provided either by the use of pollutants (p_t) or through the stock of available abatement knowledge (pollution-augmenting technological progress). Then, the productive content of pollution depends on the available public knowledge about pollution-augmenting (or abatement) techniques, which is supposed to result from the government's effort; hence $z_t = G_t p_t$, where G_t defines abatement public spending (we neglect other forms of government expenditures).[12] Thus, the firm can generate the same output by using intensively the natural resource if the abatement technology is inefficient, or—on the contrary—by using few natural resources if the pollution-augmenting technical progress is important. Fourth, we consider that $\phi = 1 - \alpha - \beta$ in order for the production function (2) to exhibit constant returns-to-scale relative to private factors (rival inputs). Nevertheless—as we will see—at the aggregate level the knowledge and public spending externalities allow obtaining an endogenous growth path because the social return of capital is constant.

In a perfect-competition decentralized economy, each firm chooses private factors (k_t, l_t, and p_t) to maximize its profit

$$\Pi_t = y_t - r_t k_t - w_t l_t - \pi_t p_t,$$

where w_t is the hourly wage rate, r_t the real interest rate, and π_t the environmental tax on polluting input—this tax can be assimilated to the price of a permit to pollute. The first-order conditions ensure that the price of factors is given by their marginal returns

[10] In our model, as we consider a continuum of representative individuals (which consists of a household and a competitive firm) whose total measure is one, the economy-wide amount of capital is the same as the aggregated amount.

[11] Consistent empirical evidence reports that the environmental quality enhances the productivity of inputs by providing non-extractive services (Van Ewijk and Van Wijnbergen, 1995; Mujan et al., 2019). According to the World Bank (1992) report, the main channel through which pollution affects productivity is based on the degradation of human health. Low environmental quality can also cause important losses of the capital stock as a consequence of extreme meteorological phenomena. Capitalizing on this work, we assume that the environmental quality affects the total factor productivity.

[12] In Bovenberg and Smulders (1995) and Fullerton and Kim (2008), abatement knowledge is defined as the stock of public spending. To cancel out this potential source of multiplicity in our model we use the flow of public spending—which equally helps simplifying the dynamics.

in production

$$r_t = \alpha \frac{y_t}{k_t}, \tag{3}$$

$$w_t = \beta \frac{y_t}{l_t}, \tag{4}$$

$$\pi_t = (1 - \alpha - \beta)\frac{y_t}{p_t}. \tag{5}$$

2.3. Preferences

The representative household starts at the initial period with a positive stock of capital (k_0), and chooses the path of consumption $\{c_t\}_{t\geq 0}$, hours worked $\{l_t\}_{t\geq 0}$, and capital $\{k_t\}_{t>0}$, such as to maximize the present discounted value of its lifetime utility

$$U = \int_0^\infty e^{-\rho t} u(c_t, l_t, Q_t)\, dt, \tag{6}$$

where $\rho \in (0, 1)$ the subjective discount rate. The instantaneous utility is assumed to be separable, namely[13]

$$u(c_t, l_t, Q_t) = \log(c_t) - \frac{1}{1+\eta} l_t^{1+\eta} + \varphi \log(Q_t),$$

where $\varphi > 0$ reflects environmental preferences, and $\eta \geq 0$ is the constant elasticity of intertemporal substitution in labour.

Households use labor income ($w_t l_t$) and capital revenues ($q_t k_t$, where q_t is the rental rate of capital), to consume (c_t) and invest ($\dot{k}_t$). They pay taxes on the wage income ($\tau_t w_t l_t$, where τ_t is the wage tax rate), hence the following budget constraint

$$\dot{k}_t = q_t k_t + (1 - \tau_t) w_t l_t - c_t. \tag{7}$$

The first-order conditions for the maximization of the household's programme give rise to the following Euler rule (with $q_t = r_t$ in competitive equilibrium)

$$\frac{\dot{c}_t}{c_t} = r_t - \rho, \tag{8}$$

and to the static relation

$$l_t^\eta = (1 - \tau_t) w_t / c_t. \tag{9}$$

[13] As previously emphasized, in contrast with e.g. Fernández et al. (2012); Bosi et al. (2015); Bosi and Desmarchelier (2018a,b) among others, our indeterminacy results do not rely on non-separable preferences. Thanks to an endogenous labor supply, complex dynamics can appear with a separable utility function.

Eq. (9) means that at each period t the marginal gain of hours worked (the net real wage $(1-\tau_t)w_t$, expressed in terms of marginal utility of consumption $1/c_t$) just equals the marginal cost (l_t^η). Finally, the optimal path of consumption has to verify the transversality condition: $\lim_{t\to+\infty}\{\exp(-\rho t)\, u'(c_t)\, k_t\}=0$.

2.4. The government

The government provides abatement expenditures (G_t) and receives taxes on labor income ($\tau_t w_t L_t$) and on polluting activities ($\pi_t P_t$), where L_t and P_t denote the economy-wide levels of labor and pollutants, respectively. It balances its budget at each point of time, hence the following instantaneous budget constraint

$$\tau_t w_t L_t + \pi_t P_t = G_t. \tag{10}$$

We shall assume that the government claims a fraction $g\in(0,1)$ of aggregate output for abatement expenditures ($G_t = gY_t$). Equilibrium can exist under the mild condition $g<1-\alpha$, that we suppose throughout the paper.

3. Equilibrium

We focus on the symmetric equilibrium in a decentralized economy in which all household-firm units behave similarly.

Definition 1. A symmetric competitive equilibrium is a path $\{C_t, L_t, K_t, Z_t, P_t, Y_t, Q_t\}_0^\infty$ that solves Eqs. (1), (2), (3), (4), (5), (8), (9) and (10), verifies the transversality condition, and satisfies the IS equilibrium $\dot{K}_t = Y_t - C_t - G_t$.

From the aggregate perspective, using Eq. (9) the labor supply is $L_t^{\eta+1} = (1-\tau_t)\beta Y_t/C_t$. Following the government's budget constraint (10), we have in equilibrium $(1-\tau_t)\beta = 1-g-\alpha$, hence

$$L_t = \left[(1-g-\alpha)\frac{Y_t}{C_t}\right]^{1/(1+\eta)}. \tag{11}$$

Thus, from (5), the level of pollutants is

$$P_t = \left(\frac{1-\alpha-\beta}{\pi_t}\right) Y_t; \tag{12}$$

hence, $Z_t = G_t P_t = g(1-\alpha-\beta)Y_t^2/\pi_t$. From Eq. (2), the aggregate production function writes

$$Y_t = A(Q_t)K_t^{\alpha+\beta}\left[(1-g-\alpha)\frac{Y_t}{C_t}\right]^{\beta/(1+\eta)} Z_t^{1-\alpha-\beta}. \tag{13}$$

Definition 2. A balanced-growth path (BGP) is a competitive equilibrium where all growing variables grow at the common (endogenous) rate γ, and the environmental quality is constant: $\gamma := \dot{C}_t/C_t = \dot{K}_t/K_t = \dot{Y}_t/Y_t = \dot{\pi}_t/\pi_t$, and $\dot{Q} = 0$.

To obtain an endogenous growth path, the environmental tax (π_t) should grow at the same rate as output along that path. To this end, following Fullerton and Kim (2008), we need to define the new ratio $\pi_{k,t} := \pi_t/K_t$ (the environmental tax per unit of capital) which is constant in the long-run. Interestingly, from Eq. (12), we derive that $P(t)/Y(t) = (1-\alpha-\beta)\pi_{k,t}/K_t$. As $\pi_{k,t}$ is constant and K_t grows at the rate γ in the long-run, it follows that the *emission intensity* measured as the the emissions per unit of output ($P(t)/Y(t)$) asymptotically declines (at the rate $-\gamma$). This feature is consistent with the well-known stylized fact in the climate change studies whereby the emission per unit economic output (such that the CO_2 emissions per unit of GDP, see the 2019 Global Carbon Budget) generally declines over time in many countries. Additionally, to obtain long-run stationary ratios, we deflate all growing variables by the capital stock (we henceforth omit time indexes), namely: $c_k := C/K$ and $y_k := Y/K$.

Using (12) and (13), we find

$$y_k = \lambda \left[A(Q) c_k^{-\beta/(1+\eta)} \right]^{1/\varepsilon} =: y_k(Q, c_k) \tag{14}$$

where $\lambda := \left[(1-g-\alpha)^{\beta/(1+\eta)} \left(g(1-\alpha-\beta)/\pi_k \right)^{1-\alpha-\beta} \right]^{1/\varepsilon} > 0$, and $\varepsilon := 1 - \beta/(1+\eta) - 2(1-\alpha-\beta) > 0$ because $\alpha > 1-\alpha-\beta$.

Relation (14) depicts an inverse relationship between the consumption and the output ratios. The intuition comes from the labor market equilibrium (9). Following an increase in the consumption ratio, the marginal utility of consumption decreases, inducing households to substitute leisure for working hours (leisure and consumption are complement in equilibrium). Then, the equilibrium labor supply and output are reduced.

The reduced-form of the model is obtained by using Eqs. (1), (3), (8), (12) and (14), namely

$$\begin{cases} \dfrac{\dot{c}_k}{c_k} = (\alpha + g - 1) y_k(Q, c_k) + c_k - \rho, & (a) \\[2ex] \dot{Q} = E(Q) - \dfrac{(1-\alpha-\beta) y_k(Q, c_k)}{\pi_k}, & (b) \end{cases} \tag{15}$$

We determine the steady-state solutions and analyze local dynamics of the model in section 4, before studying global dynamics in sections 5 and 6.

4. Long-run solutions of the model

Steady-state are computed by setting $\dot{c}_k = \dot{Q} = 0$ in (15). To obtain analytical values, we consider the usual following specifications (see Fullerton and Kim, 2008): $A(Q) = AQ^\delta$, and $E(Q) = vQ(\bar{Q} - Q)$, where $A > 0$ and $v > 0$ are scale parameters, and $\delta \in (0, 1)$ is the elasticity of productivity to the natural capital.

4.1. Existence

The following theorem establishes three regimes according to the value of the discount rate.

Theorem 1. *If $\varepsilon < \delta$, there are two critical values of the discount rate (ρ_1 and ρ_2, with $0 < \rho_1 < \rho_2$), such that the long-run equilibria are characterized by the following regimes:*

- *Regime $\mathcal{R}_1$: $\rho < \rho_1$. There is only one steady state: a "dark" equilibrium (point D), characterized by a low economic growth and a low environmental quality.*
- *Regime $\mathcal{R}_2$: $\rho > \rho_2$. There is only one steady state: a "green" equilibrium (point G), characterized by a high economic growth and a high environmental quality.*
- *Regime $\mathcal{R}_3$: $\rho_1 < \rho < \rho_2$. There are three steady states: the dark equilibrium (D), the green equilibrium (G), and an intermediate equilibrium (point M).*

Proof. See Appendix A.

The endogenous growth steady-states are given by the crossing-points of two relations between c_k and Q that are depicted in the Figure 2. Indeed, at the steady-state, the consumption ratio (c_k) and the environmental quality (Q) are constant, so that all growing variables grow at the constant rate (γ).

We restrict the analysis to strictly positive steady-states, namely $Q \in (0, \bar{Q})$ and $c_k \in (\rho, +\infty)$. The first relation is the $\dot{c}_k = 0$ locus, which—from Eq. (15a)—is denoted by $Q = \Psi(c_k)$; this relation describes an increasing continuous curve in the (c_k, Q)-plan. The second relation is the $\dot{Q} = 0$ locus, which—from Eq. (15b)—corresponds to $c_k = \Phi(Q)$; if $\varepsilon < \delta$, this relation also describes an increasing continuous curve in the (c_k, Q)-plan, with an inflexion-point reflecting a change of concavity, and a vertical asymptote at $\bar{Q}$. In this case, there are two critical values ρ_1 and ρ_2, where $0 < \rho_1 < \rho_2$, such that: (i) if $\rho < \rho_1$ there is only one crossing-point, the *dark equilibrium* (point D, in Figure 2); (ii) if $\rho > \rho_2$ there is only one crossing-point, the *green equilibrium* (point G), and (iii) if $\rho_1 < \rho < \rho_2$ there are three crossing-points: D, G, and an *intermediate equilibrium* (point M).

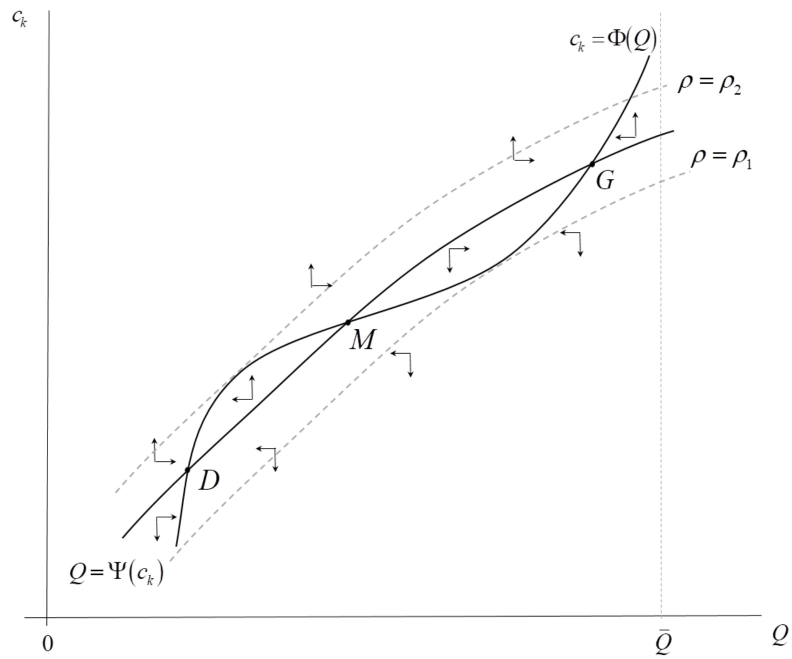

Figure 2: The phase portrait and multiplicity of BGPs

Consequently, for $\rho_1 < \rho < \rho_2$ there is a corridor that produces multiplicity (see Figure 2). Fundamentally, this multiplicity comes from the interaction between the two increasing relationships linking environmental quality and the consumption ratio.

The first relationship arises from the assumption of balanced-growth in the long run (namely $\dot{K}/K = \dot{C}/C = \gamma$). According to the Euler equation (8) and the IS equilibrium, this condition amounts to $(1-g)y_k - c_k = \alpha y_k - \rho$, or

$$c_k - \rho = (1 - g - \alpha)y_k(c_k, Q). \tag{16}$$

As we have seen, the environmental quality generates a positive externality on the output ratio y_k. The relation between c_k and Q then crucially depends on the sign of $1 - g - \alpha$. This condition is intuitive. As environmental quality increases, the growth rates of consumption ($\dot{C}/C$) and private capital ($\dot{K}/K$) increase, through a positive effect on the output ratio. The impact of the output ratio on the growth rate of consumption depends on the return of capital (α) in Eq. (8), while its impact on the growth rate of capital depends on public spending $(1-g)$. As $\alpha < 1 - g$ for a plausible calibration, the consumption ratio c_k must rise in response to an increase in Q, in order to restore the equality $\dot{K}/K = \dot{C}/C$ along the BGP; hence, the increasing function $\Psi(Q)$.

The second relationship is related to the environmental regeneration function. In the steady state, sustainable growth implies that pollution emissions are absorbed by the process of ecological regeneration, namely $P = E(Q)$. Pollution emissions positively depend on the output ratio (y_k), which is increasing in the environmental quality (Q)

and decreasing in the consumption ratio (c_k). Thus, the link between the consumption ratio and environmental quality crucially depends on the relative effect of Q on pollution emissions and on the environment absorption capacity. If $\varepsilon < \delta$, the former effect always dominates, and Q and c_k must be positively associated along the environmental equilibrium; hence, the increasing function $\Phi(Q)$.[14]

Economically, the multiplicity of long-run solutions is based on the reciprocal interaction between economic growth and the environment. A low environmental quality generates low factor productivity that impedes economic growth. Reciprocally, low economic growth means low public spending for abatement, and leads to high emission flows relative to the natural regeneration capacity. These mechanisms reverse in the case of high environmental quality, and lead to high economic growth. Therefore, there can be multiple self-fulfilling steady states, as in numerous works in the context of environmental growth models (as, e.g. Prieur, 2009; Bosi and Desmarchelier, 2018b).

However, the originality of our setup is that *three* possible balanced-growth paths can emerge in the steady state. This novelty comes from the derivative of the $\Phi(Q)$ curve that turns twice (i.e. provided that $\varepsilon < \delta$, this derivative is positive and successively increasing-decreasing-increasing). Indeed, along the stationary locus of Q (the $\Phi(Q)$ curve), the effect of a change in Q differs depending on the level of environmental quality. If Q is low, an increase in environmental quality has a major impact on the total factor productivity. If Q is high, an increase in environmental quality sharply reduces the natural absorption capacity (because $E'(Q) < 0$ at high values of Q). In both cases, pollution emissions strongly increase, so that the consumption ratio (c_k) must substantially increase to restore the environmental equilibrium. In contrast, for intermediate values of Q the effect of an increase in environmental quality on the equilibrium is moderate, because both pollution and natural absorption capacity widen (indeed, $E'(Q) > 0$ at low values of Q); thus, the consumption ratio does not need to vary much to restore the equilibrium. This explains the form of the $\dot{Q} = 0$ locus.

Whether the economy will be dragged down into the dark equilibrium—that can be assimilated to a poverty trap with low environmental quality and economic growth—or will enjoy higher environment and growth trajectories associated with points M or G, respectively, will depend on its initial location—in particular the initial environmental stock Q_0—but also on households' expectations (since c_k is a jumpable variable). This alternative exemplifies the "history versus expectation" scenario of Matsuyama (1991) and Krugman (1991), and opens the door for hysteresis as we will see.

[14]This is the more general case, because it allows exhibiting three steady states. If $\delta < \varepsilon$, $\Phi(Q)$ is depicted by a U-curve. In this case, there is still multiplicity and indeterminacy although the model gives rise to only two steady states.

4.2. Local dynamics

By linearization in the neighborhood of steady state i, $i \in \{D, M, G\}$, the system (15) behaves according to $(\dot{c}_k, \dot{Q}) = \mathbf{J}^i(c_k - c_k^i, Q - Q^i)$, where $\mathbf{J}^i$ is the Jacobian matrix. The reduced-form includes one jump variable (the consumption ratio c_{k0}) and one pre-determined variable (the environmental quality Q_0). Thus, for BGP i to be well determined, $\mathbf{J}^i$ must contain two opposite-sign eigenvalues. Using (15), we compute

$$\mathbf{J}^i = \begin{pmatrix} CC^i & CQ^i \\ QC^i & QQ^i \end{pmatrix},$$

where,

$$CC^i = (\alpha + g - 1)c_k^i y_{kc}^i + c_k^i > 0, \tag{17}$$

$$CQ^i = (\alpha + g - 1)c_k^i y_{kQ}^i < 0, \tag{18}$$

$$QQ^i = E'(Q) - y_{kQ}^i(1 - \alpha - \beta)/\pi_k < 0, \text{if } \varepsilon < \delta \tag{19}$$

$$QC^i = -y_{kc}^i(1 - \alpha - \beta)/\pi_k > 0, \tag{20}$$

with $y_{kc}^i := \frac{\partial y_k^i}{\partial c_k^i} = -\left(\frac{\beta}{(1+\eta)\varepsilon}\right) \frac{y_k^i}{c_k^i} < 0$, and $y_{kQ}^i := \frac{\partial y_k^i}{\partial Q^i} = \left(\frac{\delta}{\varepsilon}\right) \frac{y_k^i}{Q^i} > 0$.

The following theorem establishes the topological behaviour of each steady-state.

Theorem 2. *(Local Stability) The BGPs D and G are locally determinate (saddle-point stable), and M is locally indeterminate (stable) or unstable.*

Corollary 1. *Regarding the local stability of $M(c_k^M, Q_k^M)$, a Hopf bifurcation arises at $\pi_k = \pi_k^h$, where π_k^h is defined by*

$$\pi_k^h = \left(\frac{\delta}{\varepsilon}\right) \frac{y_k^M(1 - \alpha - \beta)}{Q^M[E'(Q^M) + CC^M]} > 0.$$

Proof. See Appendix B.

Theorem 2 shows that the three steady states can be relevant. Furthermore, from corollary 1, the dynamics in the vicinity of the point M can exhibit cyclical properties. It results that further investigations are needed to establish the short- and long-run behavior of the economy from a global dynamics perspective. Beforehand, the following section performs a quantitative analysis showing that the different regimes and the Hopf bifurcation arise for realistic parameters' and variables' values.

5. A quantitative assessment

To establish numerical results, we use the following calibration of the model. Regarding the households' behavior, the discount rate is scanned over the range $(0.001, 0.03)$, with $\rho = 0.01$ in the baseline calibration (corresponding to the long-run value of the risk-free interest rate used e.g. in Stern, 2006). The labor elasticity of substitution is fixed at $\eta = 0$, thus characterizing an infinite Frisch elasticity, as usual in business cycle models (see e.g. Schmitt-Grohé and Uribe, 1997). The preference parameter φ—which affects only the welfare—will be scanned over a large range of values.

Regarding the technology, we fix $A = 1$ to obtain realistic rates of economic growth; the elasticity of output to physical capital is set to represent the capital-share in GDP, namely $\alpha = 0.26$, and the elasticity to human capital is set to $\beta = 0.6$ in our baseline calibration. The corresponding elasticity relative to the polluted input is $\phi = 0.14$. This elasticity is higher that the one that would result from a neoclassical growth model based on an exogenous total factor productivity; in such a model—according to the cost-share theorem—the GDP elasticity of energy should lie between 0.025 and 0.1 on average, because the observed environmental taxes-to-GDP ratio is low (for example, about 2.5 % of GDP in the European Union). However, economists and historians underlined that the role of energy in economic growth could be much higher than that assigned by the cost-share theorem (see e.g. Georgescu-Roegen, 1971; Costanza, 1980; Murphy and Hall, 2011, and Stern, 2011, for a survey); for example, using an error correction model, Giraud and Kahraman (2014) find a long-run GDP elasticity of energy between 0.6 and 0.7. Therefore, we choose an intermediate value $\phi = 0.14$, slightly below the one (0.1875) used by Fullerton and Kim (2008), because in our model labor is endogenous.

Regarding the government's behavior, the public spending ratio is fixed to its historical average in OECD countries ($g = 0.25$). The corresponding (endogenous) tax rate on wages is 0.18, close to the data for developed countries (0.16 on average in OECD countries over the period 2000-2019).

Regarding the environment side, on the balanced-growth equilibrium path the value of $\pi_k := \pi_t/K_t$ is the ratio of two growing variables. This parameter will be scanned over a large range of values to verify the presence of bifurcations, with $\pi_k = 2$ in the baseline calibration. Similarly, the value of v in the natural regeneration process will be scanned over a large range, and in the baseline calibration we adopt the value $v = 0.04$ chosen in Fullerton and Kim (2008) from Nordhaus (1994). Finally, $\bar{Q}$ is normalized to unity, and the elasticity of the natural externality in the production function is fixed to $\delta = 0.5$.

PARAMETERS		
Households		
ρ	0.001 to 0.03	Discount rate (0.01 in the baseline calibration)
η	0	Labor elasticity of substitution
φ	0 to 100	Environmental preference parameter
Technology		
A	1	Total productivity parameter
α	0.26	Physical capital elasticity in the production function
β	0.6	Labor elasticity in the production function
ϕ	0.14	Polluting-input elasticity in the production function
Government		
g	0.25	Government spending
π_k	0.1 to 50	Pollution tax (2 in the baseline calibration)
Environment		
v	0.01 to 0.2	Natural regeneration process (0.04 in the baseline calibration)
$\bar{Q}$	1	Maximal environmental level
δ	0.5	Elasticity of the natural externality in the production function

Table 1: Baseline calibration

5.1. Equilibria and bifurcations

Formally, our model exhibits two (codim 1) *saddle-node bifurcations* at $\rho = \rho_1$ and $\rho = \rho_2$.[15] In our baseline calibration, these values are $\rho_1 \simeq 0.00993$ and $\rho_2 \simeq 0.01065$, respectively. To organize the discussion, let us define the function $f(Q) := \Phi(Q) - \Psi^{-1}(Q)$, such that the steady-state solutions are defined by $f(Q) = 0$. As depicted in Figures 3, at $\rho = \rho_1$ points M and G collide (*saddle-node bifurcation* SN_1, Figure 3d): for closely lower value of ρ, equilibria M and G disappear and the system switches from regime $\mathcal{R}_3$ to regime $\mathcal{R}_1$ (Figure 3a). At $\rho = \rho_2$ points D and M collide (*saddle-node bifurcation* SN_2, Figure 3f): for closely higher value of ρ, equilibria D and M disappear and the system switches from $\mathcal{R}_3$ to $\mathcal{R}_2$ (Figure 3c). If one authorizes another parameter to vary (say, π_k), we obtain a (codim 2) *cusp* bifurcation (as in Figure 3b), such that points M, D, and G collide. This bifurcation is obtained at $(\rho, \pi_k) \simeq (0.01196, 2.625)$, when $f(Q) = 0$ at the inflexion-point.

The *cusp* point is interesting, because it allows organizing the dynamics. As shown by Figures 3, regime $\mathcal{R}_2$ characterizes a situation where the unique equilibrium (G) is

[15] The codimension of a bifurcation is the number of parameters that must be varied to generate the bifurcation.

located above the inflexion-point of $f(Q)$, while regime $\mathcal{R}_1$ characterizes a situation where the unique equilibrium (D) is located below this inflexion-point.

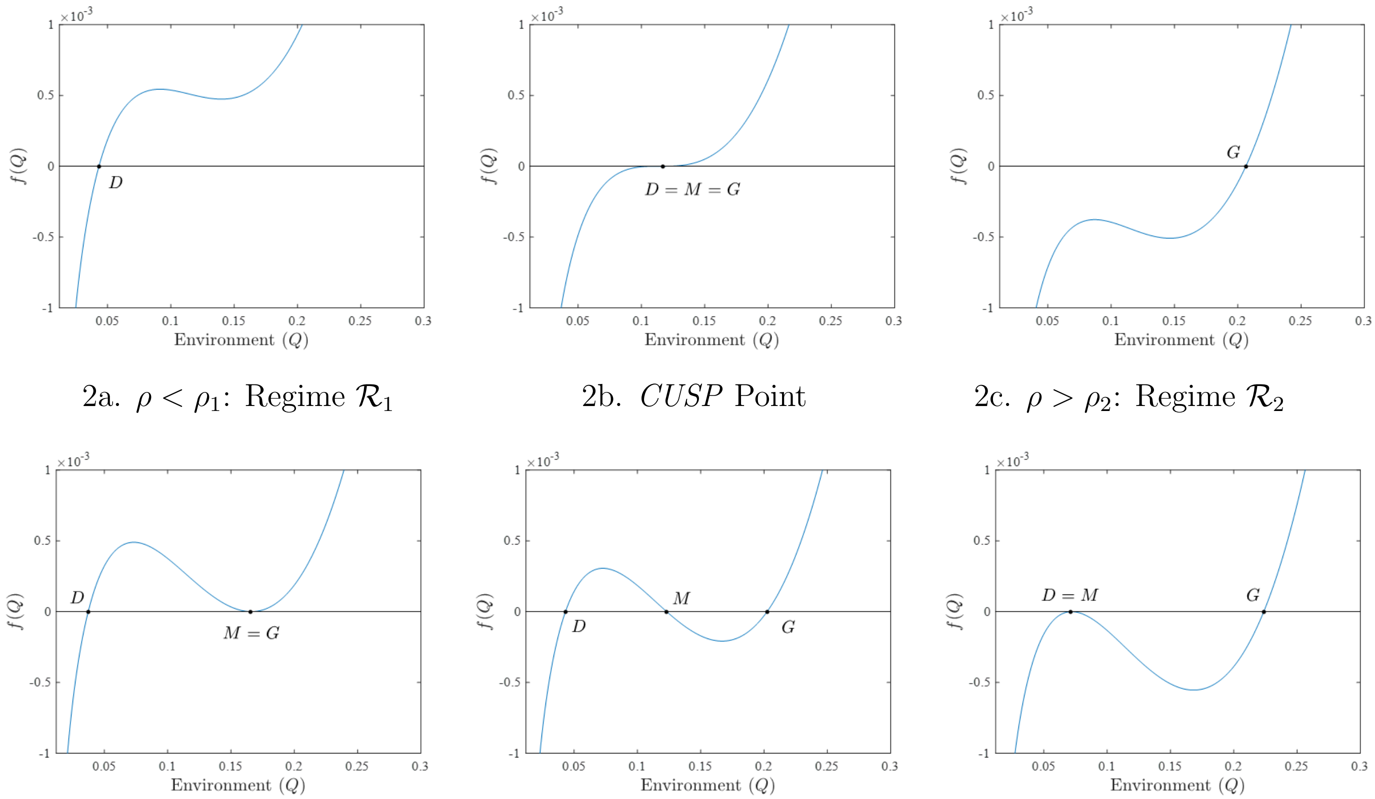

2a. $\rho < \rho_1$: Regime $\mathcal{R}_1$

2b. *CUSP* Point

2c. $\rho > \rho_2$: Regime $\mathcal{R}_2$

2d. $\rho = \rho_1$: Bifurcation SN_1

2e. $\rho_1 < \rho < \rho_2$: Regime $\mathcal{R}_3$

2f. $\rho = \rho_2$: Bifurcation SN_2

Figure 3: Topological Regimes

5.2. Hysteresis

The occurrence of a *cusp* singularity can generate a hysteresis phenomenon as described in Figure 4, which depicts the steady-state loci when the environmental tax π_k changes. Suppose e.g. that the economy is initially located at point A in the green steady state G associated to $\pi_k = \pi_2$. If π_k decreases until π_1, the economy moves—along the curve of type-G steady states—until point LP_1. If π_k further decreases, the economy switches to Regime $\mathcal{R}_1$ and the steady state suddenly jumps from G to the dark equilibrium D (at point B). However, if—from this point—π_k increases, the economy does not return to a green steady-state G, but environmental quality increases along the curve of type-D steady states until point LP_2 at $\pi_k = \pi_2$. If the value of π_k further increases, the economy switches to Regime $\mathcal{R}_2$ and the steady state suddenly jumps to G (at point A).

Hence, for very small changes of the environmental tax rate, the steady state can warp in a non-reversible way: decreasing too much the environmental tax rate may condemn the economy to an *irreversible* steady state with low environmental quality (the "environmental trap"). Of course, such an analysis is only based on comparative statics of the steady states, and must be further investigated from a dynamic perspective (this is the goal of section 6). Indeed, if $\pi_1 < \pi_k < \pi_2$, the three steady states are virtually reachable.

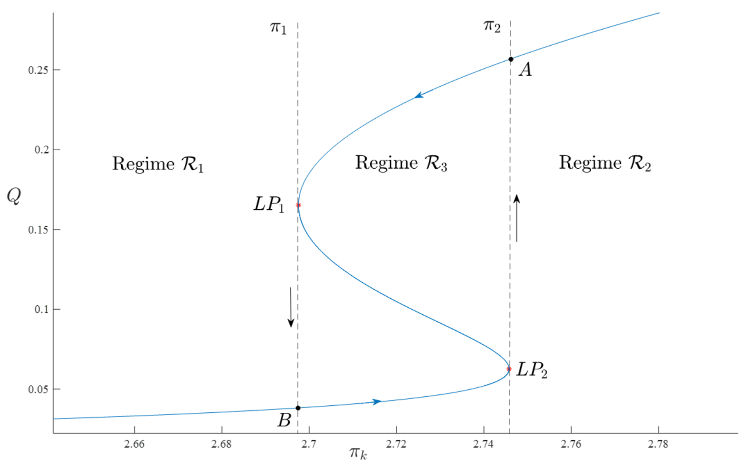

Figure 4: Environmental quality and the pollution-tax

From a policy perspective, this feature provides mixed results.[16] On the one hand, if the economy is initially located in the neighborhood of point B, the environmental policy must be handled with care. Indeed, increasing the anti-pollution tax can generate indeterminacy by switching the economy from Regime $\mathcal{R}_1$ to Regime $\mathcal{R}_3$, with the risk of generating large aggregate fluctuations, as we will see. On the other hand, a large increase in the pollution tax—from $\pi_k < \pi_1$ to $\pi_k > \pi_2$—would likely allow the economy to escape the environmental trap and move on the "green" steady state (or on a path that leads to this steady state). This opportunity pleads in favor of a "big push" in anti-pollution taxes, and calls for the adoption of tight taxation policies of the polluting input ($\pi_k > \pi_2$). However, serious difficulties could arise in the implementation of such a measure, because high environmental taxes are likely to generate social conflicts. First, since environment is a public good, environmental policies involve continuous struggles over *implicit* property rights, because property rights on natural resources—such as air or water—are often poorly defined; this makes it difficult to solve conflicts, since the taxes associated with these implicit property rights can be misunderstood by citizens. Second, environmental policies can generate intergenerational conflicts arising between both the generations alive at the time the society imposes the regulation, and the generations

[16] Using Eq. (6) we can rank the equilibria according to the long-run welfare, namely $D \prec M \prec G$, where $\prec$ denotes the usual preference relation (numerical computations are available upon request). Therefore, in Figure 4 the higher the environmental quality, the higher the long-run welfare.

alive at different times (see e.g. Karp and Rezai, 2014). More generally, since households can be characterized by a high degree of "fiscal fatigue" (Ghosh et al., 2013) notably in high-tax countries, tight environmental policies could be difficult to implement—thus plunging the economies towards the bad environmental trap.

5.3. Codim-2 bifurcations

Figure 5 synthesizes the different regimes in the (ρ, π_k)-plane. The two saddle-node bifurcations are depicted by the curves $\mathcal{SN}_1$ and $\mathcal{SN}_2$ that represent the limit-points between regimes $\mathcal{R}_1$ and $\mathcal{R}_3$, and $\mathcal{R}_3$ and $\mathcal{R}_2$, respectively. The *cusp* point (labelled CP) occurs at the intersection of these two bifurcation curves, such that—for higher levels of the discount rate or lower values of the environmental tax—regime $\mathcal{R}_3$ vanishes. Regime $\mathcal{R}_1$ arises below the lower branch that joins the *cusp* point, namely if $\rho < \rho^c$ and π_k is low enough. Regime $\mathcal{R}_2$ appears above the upper branch that joins the *cusp* point, namely if $\pi_k > \pi_k^c$ and ρ is high enough. If $\pi_k < \pi_k^c$ and $\rho > \rho^c$, regimes $\mathcal{R}_1$ or $\mathcal{R}_2$ can emerge depending on the size of these parameters. In all of these configurations, the long-run steady-state is unique (and well determinate, as we have seen). In contrast, for values of π_k and ρ located inside the two branches that join the *cusp* point, there is multiplicity because three steady states emerge (Regime $\mathcal{R}_3$). In Figures 5, the curve $\mathcal{H}$ depicts the locus of Hopf bifurcations.

Additionally to the *cusp* bifurcation, our numerical analysis highlights two other kinds of codim-2 bifurcations. The first kind is a *Bogdanov-Takens* (BT) bifurcation. In a two (or more) parameter system, such a bifurcation occurs when a Hopf bifurcation and a saddle-node bifurcation coincide in a single point of the parameter space. In Figure 5, it appears at the tangency point of a saddle-node curve $\mathcal{SN}$ and a Hopf-curve $\mathcal{H}$. As we will see, the main interest of the BT bifurcation is the presence of a homoclinic orbit—a path that connects a steady state with itself. In our model, as there are two possible saddle-node bifurcations, the BT bifurcation can appear either (i) when steady-states L and M collide, namely at point BT_1 on the curve $\mathcal{SN}_1$ (Figure 5a), or (ii) when steady-states G and M collide, namely at point BT_2 on the curve $\mathcal{SN}_2$ (Figure 5b). These two configurations crucially depend on the regeneration-efficiency parameter (v): if v is "high" ($v = 0.12$ in Figure 5a) the BT bifurcation is located at point BT_1, while it appears at point BT_2 if v is "low" ($v = 0.04$ in Figure 5b).

Furthermore, a second kind of codim-2 bifurcation can appear in the second case. As emphasized in Corollary 1, a (codim-1) Hopf bifurcation emerges in the neighborhood of the intermediate steady-state M. This bifurcation is supercritical—generating a stable limit cycle—if the first Lyapunov coefficient is negative; or subcritical—generating an unstable closed orbit—if the coefficient is positive. A codim-2 *Generalized (Bautin) Hopf* bifurcation appears at the limit case—when the first Lyapunov coefficient is zero. Based on a very wide set of numerical simulations, we find that such a bifurcation appears only in the vicinity of the BT_2 bifurcation (as at point GH in Figure 5b), ensuring in this configuration the presence of stable limit cycles for nearby parameter values.

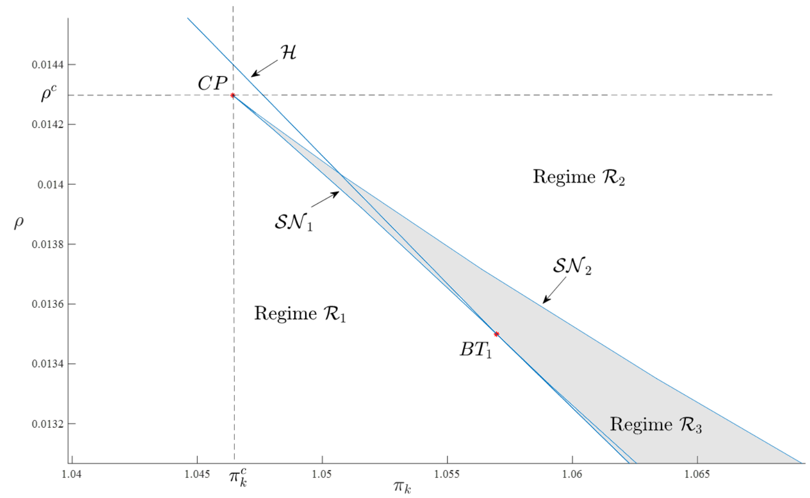

5a. $v = 0.12$

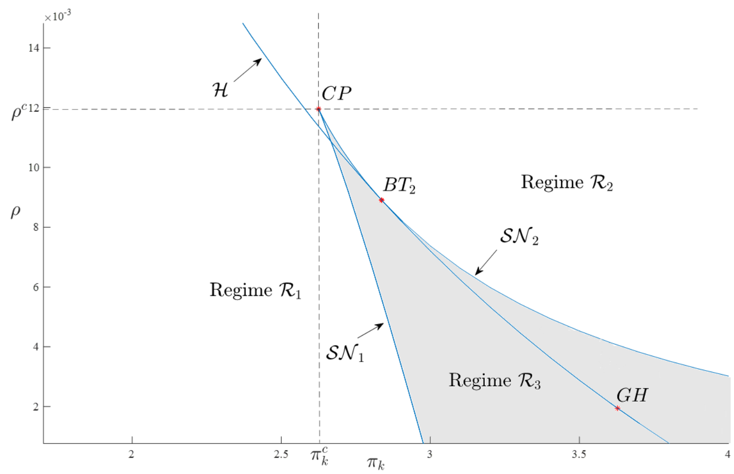

5b. $v = 0.04$

Figure 5: Bifurcation points as a function of the parameters (π_k, ρ)

Since the parameter v has crucial implications on dynamics, Figure 6 depicts the different codim-2 bifurcations as a function of parameters v and π_k in the (Q, γ) plane. The $\mathcal{H}$ curve still represents the locus of Hopf bifurcations, while the $\mathcal{LP}$ curve depicts the locus of limit-points. Clearly, CP, GH, and BT bifurcations occur for realistic values of economic growth, namely between 0 and 3%.

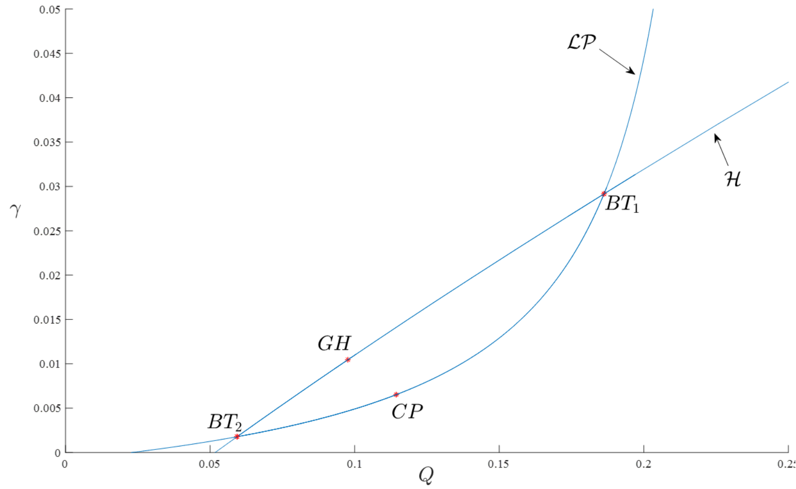

Figure 6: Codim-2 bifurcation points as a function of the parameters υ and π_k

6. Global dynamics

Having established the realism of the various bifurcations, we now analyze their implications on the global dynamics of the economy, and their consequences on the trajectories of environmental quality and pollution. Depending on the initial value of the environmental quality and households' expectations, many scenarios can appear: the economy can be trapped in the environmental-poverty trap, or experiment large oscillating trajectories leading—among others—to a possible EKC or ELC. In the following, we detail the global dynamics in the neighborhood of the *cusp* and the *BT* bifurcations, respectively.

6.1. Non-oscillating dynamics

In the vicinity of the *cusp* bifurcation, there are one or three long-run equilibria. In the last case, global indeterminacy arises. Depending on the topological nature of the intermediate equilibrium (M), two configurations can occur as states the following proposition.

Proposition 1. *Around the cusp bifurcation, indeterminacy arises as follows:*

i. *If M is unstable. For any initial environmental quality $Q_0 \in (\underline{Q}, \overline{Q})$, the economy converges towards the green or the dark equilibria (global indeterminacy).*
ii. *If M is stable. For any initial environmental quality $Q_0 \in (Q^D, Q^G)$, the three equilibria can be reached (local and global indeterminacy).*

Proof. The proof is based on a graphical analysis (see Figure 7).

If M is unstable there are two environmental quality thresholds ($\underline{Q} > Q^D$ and $\overline{Q} < Q^G$), such that—if $Q_0 < \underline{Q}$ (resp. $Q_0 > \overline{Q}$)—the initial consumption ratio c_{k0} jumps to put the economy on the saddle path that converges towards the dark (resp. green) equilibrium. If $Q_0 \in (\underline{Q}, \overline{Q})$, the two trajectories can be reached depending on the initial jump of the consumption ratio, hence the global indeterminacy of long-run equilibria. This feature characterizes the well-known *bi-stability* property associated to *cusp* points (see Figure 7a).

If M is stable, indeterminacy appears for any $Q_0 \in (Q^D, Q^G)$. Indeed, depending on the initial jump of c_{k0}, the economy can join the unique saddle path that converges to the green (resp. the dark) equilibrium, or one of the many trajectories converging to M. Consequently, there is global and local (in the vicinity of M) indeterminacy (see Figure 7b).[17]

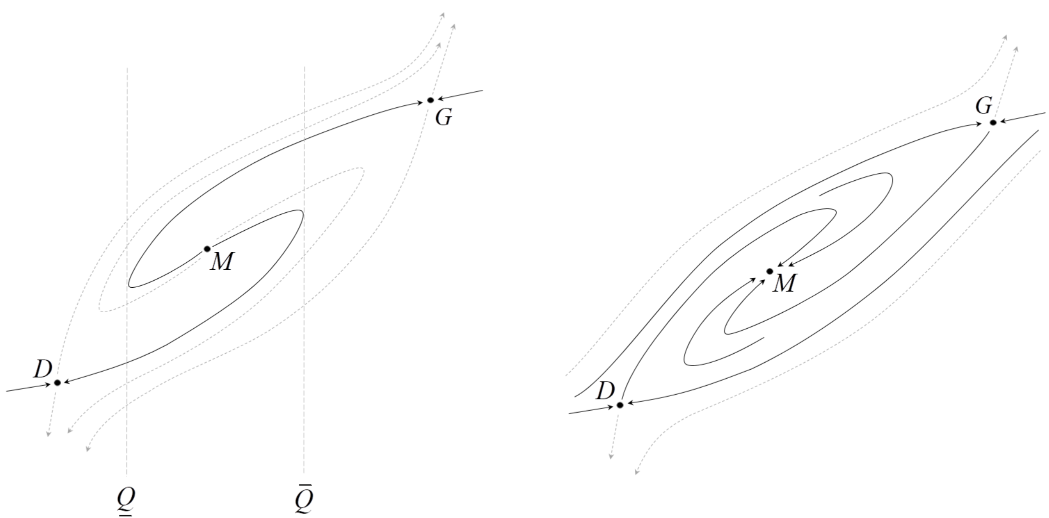

7a. Bi-stability 7b. Three long-run solutions

Figure 7: Dynamics around the *cusp* bifurcation in the (Q, c_k) plane

Proposition 1 states that the dynamics of the economy depend both on the initial environmental quality and on households' expectations (through the initial jump of the consumption ratio c_{k0}). In the case of an unstable M, the initial natural capital (Q_0) allows selecting the long-run equilibrium: if the ecosystem is initially poorly endowed in natural capital ($Q_0 < \underline{Q}$), the economy will be trapped in a region with low environmental quality and low growth. As the dark environmental equilibrium is saddle-path stable, the environment is deteriorating in an irreversible way: the economy is dragged into the environmental-poverty trap. In contrast, in the case of a high natural capital endowment

[17]Our simulations indicates the kind of parameterization that will produce an (un)stable M. By looking at Figure 5, we observe that the $\mathcal{H}$ curve (that represents the set of parameters at which a Hopf bifurcation appears) divides the (π_k, ρ)-plan into two areas. If the couple of parameters (π_k, ρ) is above (resp. below) the $\mathcal{H}$ curve, M is unstable (resp. stable). We remark that the cusp bifurcation (the CP point in Figure 5) emerges in the area where M is stable in the case 5a (i.e. $v = 0.12$), but emerges in the area where M is unstable in the case 5b (i.e. $v = 0.04$). In this way, Figure 7a (resp. 7b) depicts the global dynamics in the vicinity of the cusp bifurcation where the parameterization is given by Figure 5a (resp. 5b).

($Q_0 > \overline{Q}$), the economy will experiment the green long-run equilibrium. However, in the intermediate case ($Q_0 \in (\underline{Q}, \overline{Q})$), the two long-run scenarios can appear depending on households' expectations. In this case, the steady state is subject to "animal spirits" in the form of self-fulfilling prophecies.

Such a global indeterminacy is intuitive. Suppose e.g. that households initially expect high future environmental quality. This implies that output—through the endogenous productivity factor $A(Q)$—and the expected net return of capital will be high. Then, at the initial time households increase their savings, such that the initial consumption ratio (c_{k0}) will be low, and the initial hours worked will be high. This means that output will also be high, which generates large abatement public spending ($G_0 = gY_0$) that ensure a good environmental quality in the future. Following the same mechanism, a low expected natural capital is self-fulfilling, and may lead to the dark solution D. In other words, forward-looking households can—in equilibrium—validate any expectation on the environmental quality that can be reached in the future. Consequently, the short-run and long-run behavior of the economy depends both on *history*—the initial state of the environment Q_0—and on *expectations*—the initial jump c_{k0}.

If M is stable, global indeterminacy emerges for any initial condition ($Q_0 > 0$) depending on households' expectations, but history still plays a role in the possibility of having three reachable steady states—if $Q_0 \in (Q^D, Q^G)$—or only two—in the opposite case.

6.2. Oscillating dynamics

Global indeterminacy can also rely on long-lasting fluctuations. This is the case in the neighborhood of the Hopf bifurcation. According to Corollary 1 and Proposition 2, our model produces a (local) Hopf bifurcation at $\pi_k = \pi_k^h$ in the neighborhood of M, which gives birth of a closed orbit. As π_k moves away from π_k^h, this orbit enlarges and—at the limit—the oscillating orbit that surrounds M merges with the stable and unstable saddle-paths of D or G through a saddle-loop bifurcation, generating a homoclinic orbit. The existence of such a homoclinic orbit follows from the occurrence of a Bogdanov-Takens bifurcation. Such a BT bifurcation can occur—as previously stated—in two configurations, namely when (i) points M and G, or (ii) points M and D collapse, respectively.

Let us first consider the case (i), which arises when v is high. Based on intensive numerical simulation work, we deduce that the Hopf bifurcation is subcritical. The global dynamics is then described by the following proposition.

Proposition 2. *In regime $\mathcal{R}_3$ there is a critical initial environmental quality level $\hat{Q}$, such that indeterminacy arises as follows:*

i *If $Q_0 < \hat{Q}$, the economy is globally determinate and converges towards the dark equilibrium.*

ii *If $Q_0 \geq \hat{Q}$, the economy is globally indeterminate and can (i) jump on a closed orbit; or converge (ii) to the intermediate equilibrium, (iii) to the green equilibrium, or (iv) to the dark equilibrium, depending on households' expectations.*

Proof. The dynamics is depicted in Figure 8.

As long as $Q_0 < \hat{Q}$, the unique solution is the environmental poverty trap. If $Q_0 > \hat{Q}$, there is global indeterminacy in the different cases of Figure 8. If $\pi_k < \pi_k^h$, point M is unstable, and indeterminacy occurs because points D and G are reachable through an initial jump of the consumption ratio (Figure 8a). The subcritical Hopf bifurcation arises at $\pi_k = \pi_k^h$. If $\pi_k > \pi_k^h$, M is stable, and for values of π_k slightly higher than π_k^h there is a closed orbit that surrounds point M (Figure 8b). In this case, four long-run configurations are feasible provided that $Q_0 > \hat{Q}$: the initial jump of the consumption ratio can put the economy on saddle trajectories that converge towards D or G, respectively; on one of the multiple paths converging to M; or on the closed orbit. If π_k increases further, the closed orbit enlarges until the saddle-loop orbit that joins the stable and unstable manifolds of G (see Figure 8c). At this point, a *homoclinic orbit*—a path that connects the steady state G with itself—appears, generating a cycle of infinite amplitude.

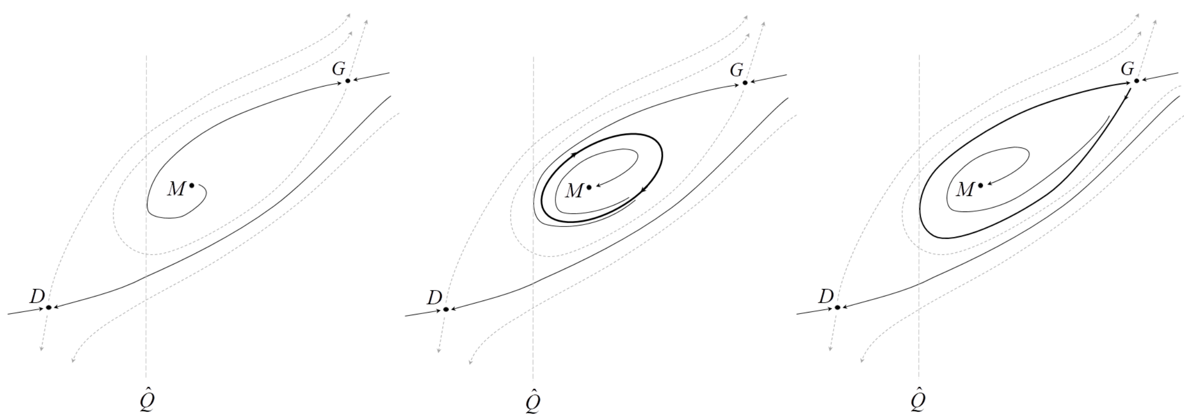

8a. $\pi_k < \pi_k^h$ 8b. $\pi_k > \pi_k^h$ 8c. The homoclinic orbit

Figure 8: Dynamics in the neighborhood of the BT_1 bifurcation in the (Q, c_k) plane

The existence of such a homoclinic orbit follows the occurrence of the BT_1 bifurcation, when the saddle-loop bifurcation and the saddle-node bifurcation SN_1 coincide, i.e. points M and G collide. Our results show that—in the neighbourhood of the BT_1 bifurcation—raising the antipollution tax is likely to generate aggregate instability. Indeed, provided that $\pi_k < \pi_k^h$ point M is unstable, and the economy converge towards the green steady state. In contrast, a tighter environmental policy may condemn the economy to locate on one of the (infinite number of) stable oscillating trajectories that lead to the intermediate steady state M. Beyond long-lasting fluctuations, increasing the pollution-tax then can generate aggregate instability by producing local indeterminacy of the transition path towards M.

Another Bogdanov-Takens bifurcation arises in the case (ii), when v is low. In this case, the Hopf bifurcation can be supercritical, because—as previously stated—there is a GH bifurcation that ensures the existence of stable limit-cycles for nearby parameters' values. This configuration occurs when steady states M and D are close to each other. Now, the homoclinic orbit connects the steady-state D with itself, and the BT_2 bifurcation occurs when the saddle-loop bifurcation and the saddle-node bifurcation SN_2 coincide in a single point of the parameter space, i.e. points M and D collide.

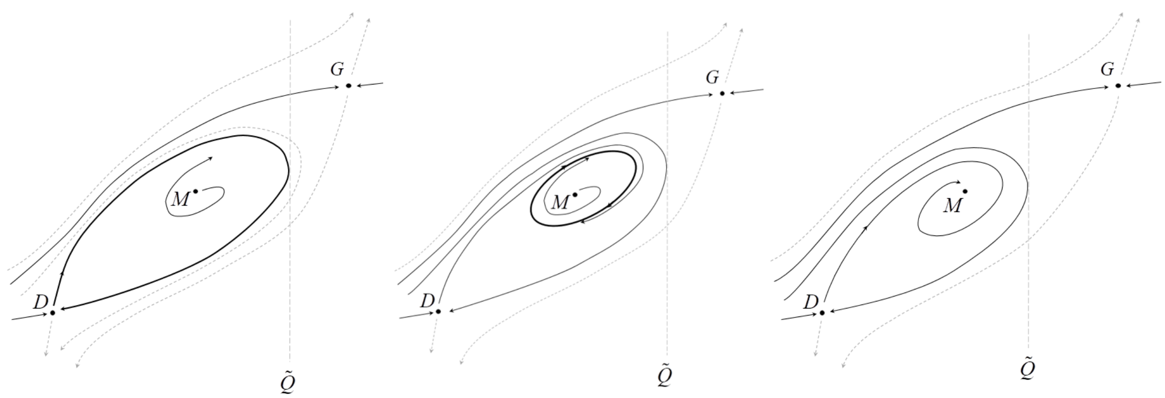

9a. The homoclinic orbit 9b. $\pi_k < \pi_k^h$ (limit cycle) 9c. $\pi_k > \pi_k^h$

Figure 9: Dynamics in the neighborhood of the BT_2 bifurcation in the (Q, c_k) plane

Compared to the first case, there are two differences. First, the closed-orbit enlarges as π_k gets lower. Second, in the case of a supercritical Hopf bifurcation, this closed-orbit is stable while point M is unstable. The initial stock of environment exerts—once again—a threshold effect. If $Q_0 > \tilde{Q}$, the economy is well-determinate and converges towards the "green" steady state. If $Q_0 < \tilde{Q}$, the economy can converge towards (i) the limit-cycle, (ii) point D, or (iii) point G, as in Figure 9b and 9c. At the limit, there is a large limit-cycle with infinite amplitude where the economy experiments long-lasting fluctuations that ultimately lead to the environmental-poverty trap (Figure 9a). From a policy perspective, results are qualitatively unchanged and this configuration once again highlights the difficulties related to environmental policies: low pollution taxes are likely to generate large fluctuations in the long run because the limit cycle enlarges; but high pollution taxes are likely to produce local indeterminacy since the steady state M becomes stable.

More generally, the emergence of two types of BT bifurcations has crucial implications on the adjustment profile of pollution, environmental quality, and economic growth, as shows the next subsection.

6.3. The time profile of pollution

In our setup, the dynamics is not predetermined—even in the absence of stochastic shocks. For the same parameter space, our model can produce a great variety of trajectories, depending on expectations and initial conditions. Let us exemplify three scenarios.

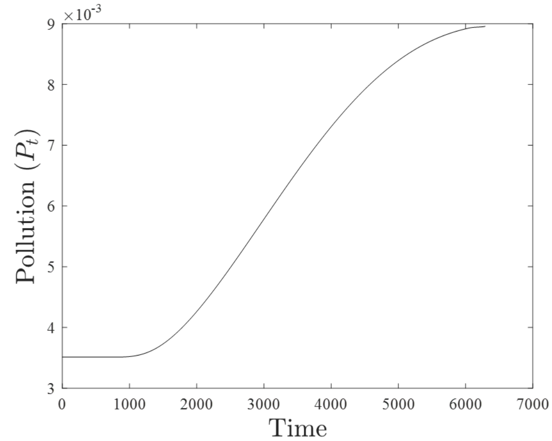

10a. Transition towards G
($\pi_k = 2.4$, $v = 0.047135$)

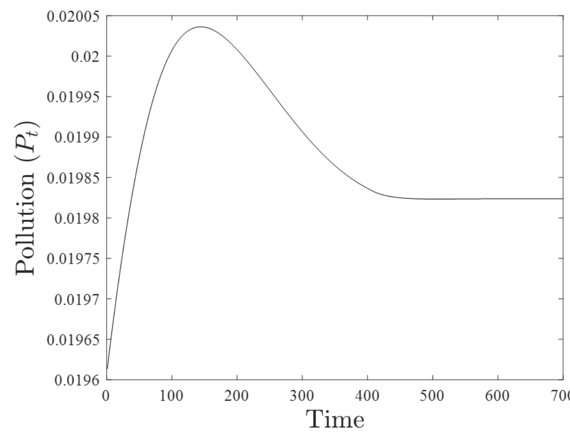

10b. Transition towards M
($\pi_k = 0.87$, $v = 0.16$)

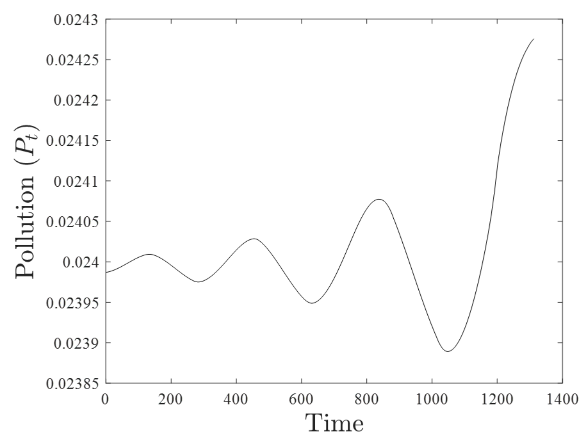

10c. Transition from M to G
($\pi_k = 0.86584$, $v = 0.16$)

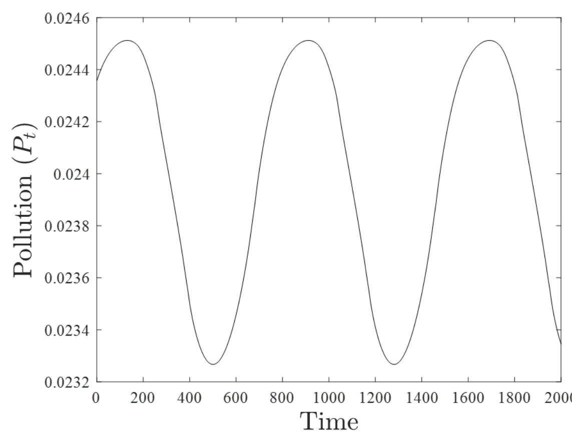

10d. Long-lasting cycle around M
($\pi_k = 0.865895$ $v = 0.16$)

Figure 10: Dynamic adjustment of pollution

(1) The first scenario describes an **Environmental Logistic Curve (ELC)**. This happens when the economy is initially located in the neighborhood of the dark or the medium equilibria, and converges towards the green steady state. Along the transition path, pollution increases first exponentially, and its growth rate decreases as the economy

gets closer to the green steady state, as depicted in Figure 10a.[18]

(ii) The second scenario depicts **pollution cycles**. These endogenous cycles appear for parameters' values close to the Hopf bifurcation, when the economy is initially located in the neighborhood of the intermediate steady state. If this steady state is unstable and the Hopf bifurcation is subcritical, during the convergence toward the green steady state pollution and economic growth are characterized by oscillating dynamics, as in Figure 10c. If M is stable and/or the Hopf bifurcation is supercritical, for some initial jump of the consumption ratio the economy can initially join the closed orbit around the intermediate equilibrium, or converge towards the limit cycle. In this case, pollution is characterized by long-lasting cyclical fluctuations (Figure 10d). Interestingly, our model leads to long-run environmental cycles without the need of exogenous perturbations; indeed, the cycles that we illustrate are not based on responses to exogenous stochastic shocks but on endogenous fluctuations resulting from the interaction between the environmental quality and the consumption ratio.

(iii) The third scenario describes an **environmental Kuznets curve**. This scenario arises in two opposite configurations. First—as previously stated—at the BT_1 bifurcation there is a homoclinic orbit that joins the green steady state to itself. Inside this homoclinic orbit all trajectories lead to the intermediate steady state M, revealing—for parameters close to the BT_1 bifurcation—an inverted U-shaped pollution profile as shown in Figure 10b. At the limit—on the homoclinic orbit—the economy can escape the intermediate steady-state: departing from G, the environmental quality initially declines, then reaches a turning point, and finally increases until the economy returns to the green steady state, as in Figure 8c. In this configuration, the endogenous environmental cycle takes a large amplitude, with an infinite periodic orbit.

This optimistic scenario can degenerate into a very undesirable situation for nearby parameters' values. Indeed, another configuration may appear if the economy departs initially from the neighborhood of the green equilibria but cannot return to this steady state. For example, if households are "pessimistic", the economy will not reach the homoclinic orbit but—through the initial jump of the consumption ratio—will locate on the path that joins the dark steady state, as in Figure 8c. Then, the economy will be condemned to the environmental poverty trap in the long run. Interestingly, an EKC of pollution does appear during the transition towards the dark equilibrium, despite the irreversible degradation of the environment. Hence, in contrast with Dasgupta et al. (2002), the potential irreversibility of environmental damages does not necessarily play against the existence of the EKC.

[18] The simulations in Figure 10 depict the time profile of polluting emissions (P_t). However, the notion of ELC (or EKC) is based on a S-shaped (or an inverted-U-shaped) curve between the polluting emissions and the economic development, measured through the log of per capita GDP. In our model, the log of per capital GDP ($\log(Y_t)$) linearly increases in all steady state (as $\partial \log(Y_t)/\partial t = \dot{Y}_t/Y_t = \gamma > 0$); hence the profile of pollution relative to (the log of) GDP—that correspond *stricto sensu* to the ELC or EKC—is similar to the profile of pollution in time.

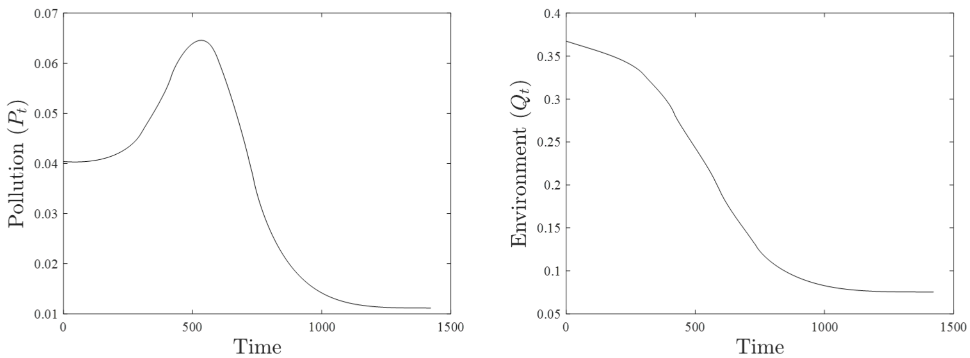

($\pi_k = 0.9$, $v = 0.16$)
Figure 11: An EKC during the transition towards the dark steady state

The important feature of Figure 11 compared to Figure 8c is that the environmental quality does not recover (after time $t = 600$), despite the reduction in emissions. Indeed, the weakening of polluting emissions comes from the weakening of economic growth, and—in equilibrium—low growth does not allow financing enough abatement expenditures to circumvent emissions (however weak may them be).[19]

7. Conclusion

This paper has shown that the dual interaction between the optimal saving behavior of households and the law of motion of the environment gives rise to complex dynamics in which environmental degradation affects economic growth. In particular, our analysis provided two important results.

On the one hand, by exhibiting multiple equilibria we offered new insights on ecological poverty traps. Following the seminal paper of Azariadis and Drazen (1990), numerous studies attempted to explain the emergence of such traps (see Xepapadeas, 1997; Azariadis and Stachurski, 2005; Antoci et al., 2011, among others). In most studies, ecological poverty traps result from exogenous threshold externalities affecting production of abatement knowledge technology (see, e.g., Xepapadeas, 1997; Prieur, 2009). In contrast, our model does not rest upon such exogenous technological breaks, and the mechanism giving birth to trapping regions is linked to the reciprocal interaction between economic growth and environment.

On the other hand, the local and global indeterminacy that we unveiled contributes to our understanding of the observed heterogeneities across countries in the time profile of emissions (López-Menéndez et al., 2014). As illustrated by our analysis, economies

[19]The EKC-like profile of pollution during a phase of environmental degradation could be illustrated by the case of some Sub-Saharan African countries—such as the Democratic Republic of Congo, Cameroon, Ivory Coast, or Nigeria—that were trapped into a no-growth equilibrium with both declining emissions and deteriorating environmental quality during the 1990s.

characterized by very close initial conditions can converge towards different equilibria in the long-run (global indeterminacy), or towards the same equilibrium with different trajectories (local indeterminacy). Consequently, our simple two-dimensional dynamic system with usual hypotheses can allow replicating a large variety of dynamics in the relationship between environment and economic growth, including the popular EKC or ELC, or long-lasting environmental cycles.

From a policy perspective, our model calls for a careful use of fiscal instruments—such as the anti-pollution tax—since bifurcations with irreversible processes may emerge for small changes in the parameters. More broadly, the environmental policy must appropriately deal with households' expectations with the aim of coordinating their behavior for reaching the desirable steady state.

There is little doubt that the analysis of the non-linear dynamics in environmental growth models deserves future research. First, based on the methodology of Barnett and Chen (2015), empirical tests could be mobilized to assess the presence of multiple equilibria and bifurcations in the CO2 emissions trajectories. Second, fruitful extensions of the model would relax the balanced-budget rule hypothesis by authorizing debt-financing of abatement expenditure as in Boly et al. (2019), for example. In these lines, the literature could capitalize on the approach of Bosi and Desmarchelier (2019) to further investigate the growth-environment relationship in higher dimensional models.

References

Antoci, A., Galeotti, M., Russu, P., 2011. Poverty trap and global indeterminacy in a growth model with open-access natural resources. Journal of Economic Theory 146, 569–591.

Arrow, K., Bolin, B., Costanza, R., Dasgupta, P., Folke, C., Holling, C., Jansson, B.O., Levin, S., Mäler, K.G., Perrings, C., Pimentel, D., 1995. Economic growth, carrying capacity, and the environment. Ecological Economics 15, 91–95.

Azariadis, C., Drazen, A., 1990. Threshold externalities in economic development. The Quarterly Journal of Economics 105, 501–526.

Azariadis, C., Stachurski, J., 2005. Poverty traps. Handbook of economic growth 1, 295–384.

Barnett, W.A., Chen, G., 2015. Bifurcation of macroeconometric models and robustness of dynamical inferences. Foundations and Trends in Econometrics 8, 1–144.

Benhabib, J., Schmitt-Grohé, S., Uribe, M., 2001. The perils of Taylor rules. Journal of Economic Theory 96, 40–69.

Boly, M., Combes, J.L., Combes-Motel, P., Menuet, M., Minea, A., Villieu, P., 2019. Public debt versus environmental debt: What are the relevant tradeoffs? Mimeo .

Bosi, S., Desmarchelier, D., 2018a. Limit Cycles Under a Negative Effect of Pollution on Consumption Demand: The Role of an Environmental Kuznets Curve. Environmental and Resource Economics 69, 343–363.

Bosi, S., Desmarchelier, D., 2018b. Natural cycles and pollution. Mathematical Social Sciences 96, 10–20.

Bosi, S., Desmarchelier, D., 2019. Local bifurcations of three and four-dimensional systems: A tractable characterization with economic applications. Mathematical Social Sciences 97, 38–50.

Bosi, S., Desmarchelier, D., Ragot, L., 2015. Pollution effects on labor supply and growth. International Journal of Economic Theory 11, 371–388.

Bovenberg, A.L., Smulders, S., 1995. Environmental quality and pollution-augmenting technological change in a two-sector endogenous growth model. Journal of Public Economics 57, 369–391.

Brock, W., Scott Taylor, M., 2010. The Green Solow model. Journal of Economic Growth 15, 127–153.

Carbon Dioxide Information Analysis Center, 2014. Fossil-fuel CO2 Emissions. http://cdiac.ornl.gov/trends/emis/meth_reg.html .

Costanza, R., 1980. Embodied energy and economic valuation. Science 210, 1219–1224.

Dasgupta, P., 1982. The control of resources. Harvard University Press., Harvard.

Dasgupta, S., Laplante, B., Wang, H., Wheeler, D., 2002. Confronting the environmental kuznets curve. Journal of Economic Perspectives 16, 147–168.

Dinda, S., 2005. A theoretical basis for the environmental Kuznets curve. Ecological Economics 53, 403–413.

Durlauf, S.N., Johnson, P.A., Temple, J.R., 2005. Growth Econometrics, in: Aghion, P., Durlauf, S.N. (Eds.), Handbook of Economic Growth. Elsevier. volume 1. chapter 8, pp. 555–677.

Fernández, E., Pérez, R., Ruiz, J., 2012. The environmental Kuznets curve and equilibrium indeterminacy. Journal of Economic Dynamics and Control 36, 1700–1717.

Foster, B., 1973. Optimal capital accumulation in a polluted environment. Southern Economic Journal 39, 544–547.

Fullerton, D., Kim, S.R., 2008. Environmental investment and policy with distortionary taxes, and endogenous growth. Journal of Environmental Economics and Management 56, 141–154.

Georgescu-Roegen, N., 1971. The Entropy Law and the Economic Process.

Ghosh, A.R., Kim, J.I., Mendoza, E.G., Ostry, J.D., Qureshi, M.S., 2013. Fiscal fatigue, fiscal space and debt sustainability in advanced economies. The Economic Journal 123, F4–F30.

Giraud, G., Kahraman, Z., 2014. How dependent is growth from primary energy ? Output energy elasticity in 50 countries (1970-2011). Mimeo .

Grossman, G.M., Krueger, A.B., 1995. Economic growth and the environment. The Quarterly Journal of Economics 110, 353–377.

Hartman, R., Kwon, O.S., 2005. Sustainable growth and the environmental Kuznets curve. Journal of Economic Dynamics and Control 29, 1701–1736.

Heijdra, B.J., Heijnen, P., 2013. Environmental abatement and the macroeconomy in the presence of ecological thresholds. Environmental and Resource Economics 55, 47–70.

Jaunky, V.C., 2011. The CO2 emissions-income nexus: evidence from rich countries. Energy Policy 39, 1228–1240.

John, A., Pecchenino, R., 1994. An overlapping generations model of growth and the environment. The Economic Journal 104, 1393–1410.

Kaika, D., Zervas, E., 2013. The Environmental Kuznets Curve (EKC) theory—Part A: Concept, causes and the CO2 emissions case. Energy Policy 62, 1392–1402.

Karp, L., Rezai, A., 2014. The political economy of environmental policy with overlapping generations. International Economic Review 55, 711–733.

Krugman, P., 1991. History versus expectations. The Quarterly Journal of Economics 106, 651–667.

Le Kama, A.D.A., 2001. Sustainable growth, renewable resources and pollution. Journal of Economic Dynamics and Control 25, 1911–1918.

López-Menéndez, A.J., Pérez, R., Moreno, B., 2014. Environmental costs and renewable energy: Revisiting the Environmental Kuznets Curve. Journal of Environmental Management 145, 368–373.

Lucas, R.E., 1988. On the mechanics of economic development. Journal of Monetary Economics 22, 3–42.

Mäler, K.G., Xepapadeas, A., de Zeeuw, A., 2003. The economics of shallow lakes. Environmental and Resource Economics 26, 603–624.

Matsuyama, K., 1991. Increasing returns, industrialization, and indeterminacy of equilibrium. The

Quarterly Journal of Economics 106, 617–650.

de Mooij, R., Bovenberg, L., 1997. Environmental tax reform and endogenous growth. Journal of Public Economics 63, 207–237.

Mujan, I., Anelković, A.S., Munćan, V., Kljajić, M., Ružić, D., 2019. Influence of indoor environmental quality on human health and productivity - A review. Journal of Cleaner Production 217, 646–657.

Murphy, D.J., Hall, C.A., 2011. Adjusting the economy to the new energy realities of the second half of the age of oil. Ecological Modelling 223, 67–71.

Nordhaus, W., 1994. Managing the Global Common, the Economics of Climate Change. MIT Press, Cambridge.

Pérez-Suárez, R., López-Menéndez, A.J., 2015. Growing green? Forecasting CO2 emissions with environmental Kuznets curves and logistic growth models. Environmental Science & Policy 54, 428–437.

Prieur, F., 2009. The environmental Kuznets curve in a world of irreversibility. Economic Theory 40, 57–90.

Romer, P.M., 1986. Increasing returns and long-run growth. Journal of Political Economy 94, 1002–1037.

Rubio, S.J., Garcia, J.L., Hueso, J.L., 2009. Neoclassical growth, environment and technological change: The environmental Kuznets curve. The Energy Journal 143, 143–168.

Schmitt-Grohé, S., Uribe, M., 1997. Balanced-budget rules, distortionary taxes, and aggregate instability. Journal of Political Economy 105, 976–1000.

Selden, T.M., Song, D., 1994. Environmental quality and development: is there a Kuznets curve for air pollution emissions? Journal of Environmental Economics and Management 27, 147–162.

Shafik, N., 1994. Economic development and environmental quality: an econometric analysis. Oxford Economic Papers 46, 757–774.

Smulders, S., 2000. Economic growth and environmental quality, in: Folmer, H., Gabel, H. (Eds.), Principles of Environmental and Resource Economics. Edward Elgar Publishers, Cheltenham.

Sniekers, F., 2018. Persistence and volatility of Beveridge cycles. International Economic Review 59, 665–698.

Sobhee, S.K., 2004. The environmental Kuznets curve (EKC): a logistic curve? Applied Economics Letters 11, 449–452.

Solow, R., 1956. A Contribution to the Theory of Economic Growth. Quarterly Journal of Economics 70, 65–94.

Stern, D.I., 2004. The Rise and Fall of the Environmental Kuznets Curve. World Development 32, 1419–1439.

Stern, D.I., 2011. The role of energy in economic growth. Annals of the New York Academy of Sciences 1219, 26–51.

Stern, D.I., 2015. The environmental Kuznets curve after 25 years. CCEP Working Paper 1514 .

Stern, N., 2006. The economics of climate change. HM Treasury, London.

Stokey, N.L., 1998. Are There Limits to Growth? International Economic Review 39, 1–31.

Tahvonen, O., Kuuluvainen, J., 1991. Optimal growth with renewable resources and pollution. European Economic Review 35, 650–661.

Tahvonen, O., Salo, S., 1996. Nonconvexities in optimal pollution accumulation. Journal of Environmental Economics and Management 31, 160–177.

Toman, M.A., Withagen, C., 2000. Accumulative pollution, clean technology, and policy design. Resource and Energy Economics 22, 367–384.

Uzawa, H., 1965. Optimum technical change in an aggregative model of economic growth. International Economic Review 6, 18–31.

Van Ewijk, C., Van Wijnbergen, S., 1995. Can abatement overcome the conflict between environment and economic growth? De Economist 143, 197–216.

World Bank, 1992. Development and the Environment. Word Bank Report .

Xepapadeas, A., 1997. Economic development and environmental pollution: traps and growth. Structural Change and Economic Dynamics 8, 327–350.

Appendix A.

The first relation is the $\dot{c}_k = 0$ locus, which comes from Eq. (15a)

$$Q = \Psi(c_k) := \kappa_0 (c_k - \rho)^{\varepsilon/\delta} c_k^{\tilde{\beta}/\delta},$$

where $\tilde{\beta} := \beta/(1+\eta)$ and $\kappa_0 = [\lambda A^{1/\varepsilon}(1-\alpha-g)]^{-\varepsilon/\delta} > 0$. This relation describes an increasing continuous curve in the (c_k, Q)-plane, with $c_k \in (\rho, +\infty)$.

The second relation is the $\dot{Q} = 0$ locus, which comes from Eq. (15b)

$$c_k = \Phi(Q) := \frac{\kappa_1 Q^{\delta/\tilde{\beta}}}{E(Q)^{\varepsilon/\tilde{\beta}}},$$

where $\kappa_1 = \left[\left(\frac{1-\alpha-\beta}{\pi_k}\right)\lambda A^{1/\varepsilon}\right]^{\varepsilon/\tilde{\beta}}$. Considering $E(Q) = vQ(\bar{Q} - Q)$, the shape of the mapping $\Phi(Q)$ depends on the behavior of the ratio $Q^{\delta-\varepsilon}(\bar{Q} - Q)^{-\varepsilon}$.

There are three cases.

i. $\varepsilon > \delta$. The mapping $\Phi(\cdot)$ describes a U-shaped curve in the (c_k, Q)-plane, with two vertical asymptotes at 0 and $\bar{Q}$, i.e. $\Phi(0) = \Phi(\bar{Q}) = +\infty$.

ii. $\varepsilon = \delta$. The mapping $\Phi(\cdot)$ describes an increasing curve in the (c_k, Q)-plane, with $\Phi(0) = \kappa_1/(v\bar{Q})^{\varepsilon/\tilde{\beta}} > 0$ and $\Phi(\bar{Q}) = +\infty$.

iii. $\varepsilon < \delta$. The mapping $\Phi(\cdot)$ describes yet again an increasing curve in the (c_k, Q)-plane, with $\Phi(0) = 0$ and $\Phi(\bar{Q}) = +\infty$.

We thereafter focus on the case iii., since the condition $\varepsilon < \delta$ leads to the more general configuration, i.e. in which three long-run steady states can appear.

Lemma 1. *If $\varepsilon < \delta < \varepsilon + \beta/(1+\eta)$, the curve driven by the mapping $\Phi(Q)$ is first concave then convex in the (c_k, Q)-plane (see Figure 2 in the main text).*

Proof. Using $\tilde{\delta} := \delta/\tilde{\beta}$ and $\tilde{\varepsilon} := \varepsilon/\tilde{\beta}$, we compute: $\Phi''(Q) = \kappa_1 v^{-\tilde{\varepsilon}} Q^{\tilde{\delta}-\tilde{\varepsilon}-2}(\bar{Q}-Q)^{-\tilde{\varepsilon}-2} h(Q)$, with

$$h(Q) = (\tilde{\delta} - \tilde{\varepsilon})(\tilde{\delta} - \tilde{\varepsilon} - 1)(\bar{Q} - Q)^2 + 2\tilde{\varepsilon}(\tilde{\delta} - \tilde{\varepsilon})Q(\bar{Q} - Q) + \tilde{\varepsilon}(\tilde{\varepsilon} + 1)Q^2.$$

Thus, $h \in C^\infty([0, \bar{Q}])$, $h(0) = (\tilde{\delta} - \tilde{\varepsilon})(\tilde{\delta} - \tilde{\varepsilon} - 1)\bar{Q}^2 < 0$, and $h(\bar{Q}) = \tilde{\varepsilon}(\tilde{\varepsilon} + 1)\bar{Q}^2 > 0$, as $\delta - \varepsilon < \tilde{\beta}$. In addition, we have

$$h'(Q) = -2(\tilde{\delta} - \tilde{\varepsilon})(\tilde{\delta} - \tilde{\varepsilon} - 1)(\bar{Q} - Q) + 2\tilde{\varepsilon}(\tilde{\delta} - \tilde{\varepsilon})(\bar{Q} - 2Q) + 2\tilde{\varepsilon}(\tilde{\varepsilon} + 1)Q = \lambda_2 \bar{Q} - \lambda_1 Q,$$

where $\lambda_2 := -2(\tilde{\delta}-\tilde{\varepsilon})(\tilde{\delta}-\tilde{\varepsilon}-1)+2\tilde{\varepsilon}(\tilde{\delta}-\tilde{\varepsilon}) > 0$, and $\lambda_1 := -2(\tilde{\delta}-\tilde{\varepsilon})(\tilde{\delta}-\tilde{\varepsilon}-1)+4\tilde{\varepsilon}(\tilde{\delta}-\tilde{\varepsilon})-2\tilde{\varepsilon}(\tilde{\varepsilon}+1)$. There are two cases.
i. If $\rho_1 \leq 0$, then $h'(Q) > 0$ for all $Q \in (0, \bar{Q})$.
ii. If $\rho_1 > 0$, then $h'(Q) > 0 \Leftrightarrow Q < \bar{Q}(\lambda_2/\lambda_1)$. Yet, we have $\lambda_2 > \lambda_1$ such that $h'(Q) > 0$ for any $Q \in [0, \bar{Q}]$. Indeed, $\lambda_2 - \lambda_1 = 2\tilde{\varepsilon}[-\tilde{\delta}+2\tilde{\varepsilon}+1] > 0$.

Consequently, according to the Intermediate Value Theorem, there is a unique critical value $\hat{Q} \in (0, \bar{Q})$ such that $\Phi''(Q) < 0$ for $Q \in (0, \hat{Q})$, and $\Phi''(Q) > 0$ for $Q \in (\hat{Q}, \bar{Q})$.

□

Finally, as $\Psi(\rho) = 0$, $\Phi(0) = 0$, and $\Phi(\bar{Q}) = +\infty$, the loci $\dot{c}_k = 0$ and $\dot{Q} = 0$ can cross once of thrice, depending on the value of ρ. According to the Intermediate Value Theorem, there are two critical values ρ_1 and ρ_2—where $0 < \rho_1 < \rho_2$—such that:
- if $\rho < \rho_1$: there is only one crossing-point, defining the dark steady state (point D in Figure 1).
- if $\rho_1 < \rho < \rho_2$: there are three crossing-points: the green steady state (point G), the intermediate steady state (point M), and the dark steady state (point D).
- if $\rho > \rho_2$: only the green steady state exists.

Appendix B. Local stability

We show first that $QQ^i < 0$. Using Eqs. (15b) and (19), we have $QQ^i = E'(Q) - (\delta/\varepsilon)E(Q)/Q = v[(\varepsilon-\delta)(\bar{Q}-Q)-\varepsilon Q]/\varepsilon < 0$, as $\delta > \varepsilon$.

As the dynamics is characterized by a two-dimensional system, we can study the local stability of steady states by inspecting the slope of $\dot{c}_k = 0$ (the slope of $\Psi(c_k)$ in Figure 2, denoted by s_c^i) and $\dot{Q} = 0$ (the slope of $\Phi(Q)$ in Figure 2, denoted by s_Q^i) in the neighbourhood of each BGP i in the (c_k,Q)-plane.

First, using the Implicit Function Theorem we compute from Eqs. (17)-(20):
$s_c^i = -CQ^i/CC^i > 0$ and $s_Q^i = -QQ^i/QC^i > 0$.

Second, the trace and the determinant of the jacobian matrix are $\text{Tr}(\mathbf{J}^i) = CC^i + QQ^i$ and $\det(\mathbf{J}^i) = CC^iQQ^i - CQ^iQC^i = CC^iQC^i(s_c^i - s_Q^i)$. Since $CC^i > 0$ and $QC^i < 0$, we have $\det(\mathbf{J}^i) < 0$ if $s_c^i < s_Q^i$, as for the points D and G of Figure 2. At point M, $s_c^i > s_Q^i$ such that $\det(\mathbf{J}^i) > 0$, and a Hopf bifurcation emerges when $CC^i = -QQ^i$, such that $\text{Tr}(\mathbf{J}^i) = 0$.

It follows that points D and G—if they exist—are saddle-path stable because $\mathbf{J}^D$ and $\mathbf{J}^G$ contains two opposite-sign eigenvalues. If M exists, M is either stable ($\mathbf{J}^M$ contains two negative eigenvalues) or instable ($\mathbf{J}^M$ contains two positive eigenvalues). A Hopf bifurcation can occur when $CC^M + QQ^M = 0$. Corollary 1 comes directly from Eqs. (17) and (19).